Behaviour and Analytical Design of Fire Exposed Steel Structures, Insulated with Gypsum Plaster Slabs

Pettersson, Ove

1978

LUND INSTITUTE OF TECHNOLOGY · LUND · SWEDEN · 1978
DIVISION OF STRUCTURAL MECHANICS AND CONCRETE CONSTRUCTION BULLETIN 64

OVE PETTERSSON

BEHAVIOUR AND ANALYTICAL DESIGN OF FIRE EXPOSED STEEL STRUCTURES, INSULATED WITH GYPSUM PLASTER SLABS

LUND INSTITUTE OF TECHNOLOGY · LUND · SWEDEN · 1978
DIVISION OF STRUCTURAL MECHANICS AND CONCRETE CONSTRUCTION · BULLETIN 64

OVE PETTERSSON

BEHAVIOUR AND ANALYTICAL DESIGN OF FIRE EXPOSED STEEL STRUCTURES, INSULATED WITH GYPSUM PLASTER SLABS

Presented at the EUROGYPSUM Scientific and Technical Committee Seminar in Turin, 21-22 September 1978

BEHAVIOUR AND ANALYTICAL DESIGN OF FIRE EXPOSED STEEL STRUCTURES, INSULATED WITH GYPSUM PLASTER SLABS

By Ove Pettersson, Prof., Dr., Civil Engineering Department, Lund University, Lund, Sweden

A development of analytical design procedures, based on well-defined functional requirements, is an important task of the future fire research within different fields of the overall fire safety concept. Such procedures, successively replacing the present, internationally prevalent, schematic design methods, are necessary for getting an improved economy and for enabling more qualified and reliable fire safety analyses. A derivation of such analytical design systems is also in agreement with the present trend of development of the building codes and regulations in many countries towards an increased extent of functionally based requirements and performance criteria.

In the ideal case, a rational fire design methodology includes as essential components [1]

* analytical modelling of relevant processes; verification of model validation and accuracy; determination of critical design parameters,

* formulation of functional requirements, independent of choice of design process and expressed either in deterministic or probabilistic terms,

* determination of design parameter values, and

* verification by the means of a reliability analysis that the choice of safety factors leads to safety levels, which are consistent with the expressed functional requirements.

For a fire engineering design of load-bearing structures and partitions, a differentiated analytical procedure is permitted to be applied in Sweden, as one alternative, since about ten years. The procedure constitutes a direct design method based on temperature characteristics of the fully developed compartment fire as a function of the fire load density, the

ventilation of the fire compartment and the thermal properties of the structures enclosing the fire compartment. The design method is approved for a general practical use by the National Swedish Board of Physical Planning and Building [2]. For facilitating the practical application, design diagrams and tables are systematically produced, giving directly, on one hand, the design temperature state of the fire exposed structure, on the other, a transfer of this information to the corresponding design load-bearing capacity of the structure; c.f., for instance [3], [4], [5], [6].

1. Principles of an Analytical Design of Fire Exposed Structures

In a generalized summary way, an analytical design method for fire exposed structures, based on well-defined functional requirements, can be described according to Fig. 1.

The design fire load density, the fire compartment characteristics and the fire extinguishment and fire fighting characteristics constitute the basis for a determination of the design fire exposure, given as the gastemperature-time curve T-t of the fully developed compartment fire. Depending on the type of practical application, the load-bearing function of the structure can be required to be fulfilled for

* the complete fire process,
* a shortened fire process, limited by the time t_{ext}, necessary for the fire to be extinguished under the most severe conditions, or
* a shortened fire process, limited by the design evacuation time t_{esc} for the building.

Together with the structural design data, the design thermal properties and the design mechanical strength of the structural materials, the design fire exposure gives the design temperature state and the design load-carrying capacity R_d as the lowest value during the relevant fire process.

A direct comparison between the design load-carrying capacity R_d and the design load effect at fire S_d decides whether the structure can fulfil its required function or not at the fire exposure.

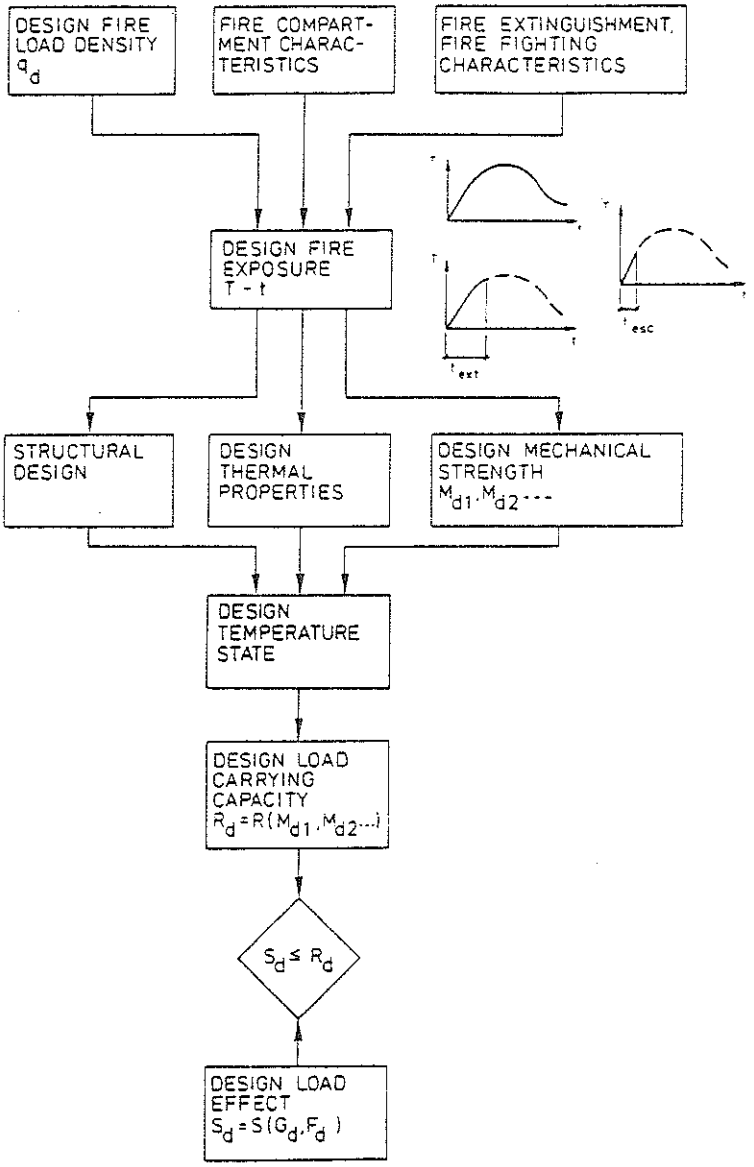

Figure 1. Procedure of an analytical design of fire exposed load-bearing structures

Following a recent draft of safety regulations [7], the determination of the design load effect S_d starts from characteristic values of permanent and variable loads G_k and F_k, connected to a defined probability of excess during a specified time period (Fig. 2). A multiplication by partial factors γ and load combination factors ψ transfers the characteristic load values to design loads G_d and F_d. The load combination factors ψ then may be differentiated with respect to whether a complete evacuation of people can be assumed or not in the event of fire. Finally, the design loads are combined and transformed to the design load effect at fire S_d.

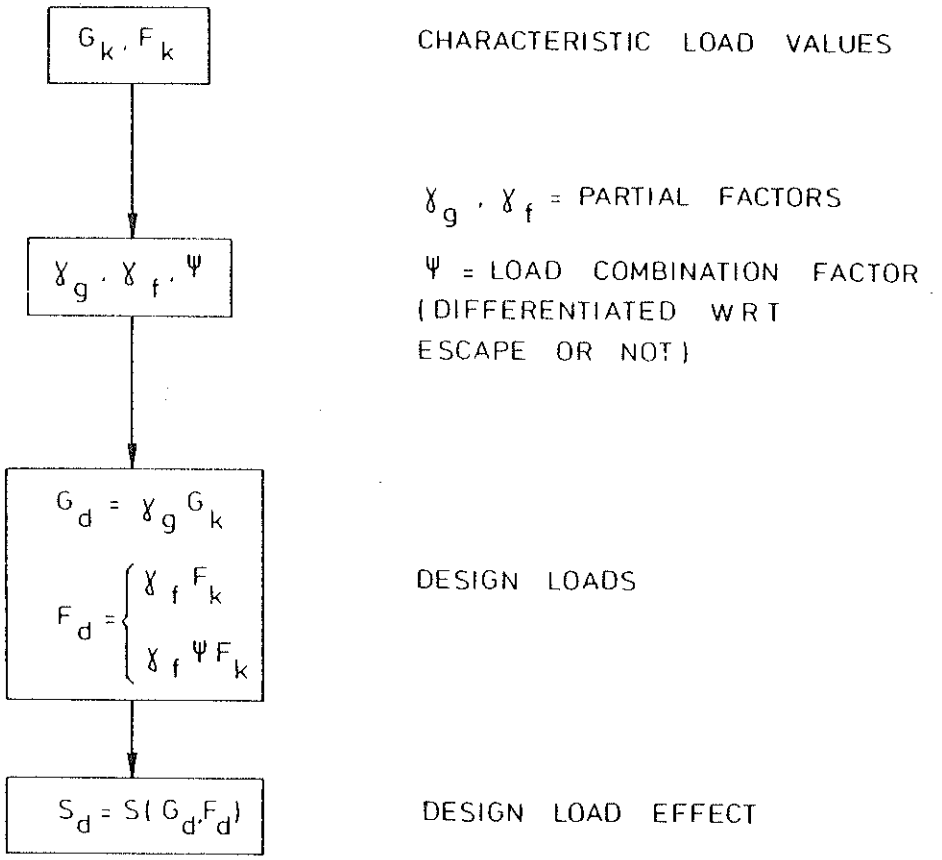

Figure 2. Procedure of determination of design load effect S_d

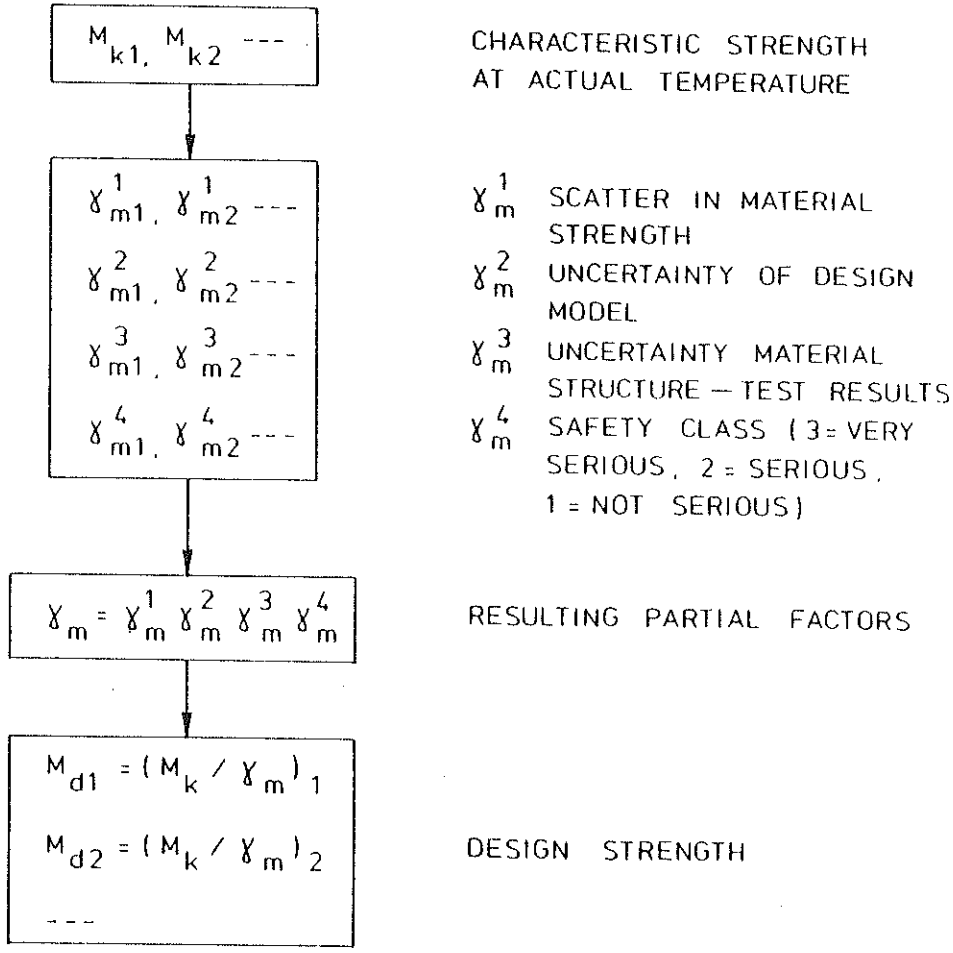

Figure 3. Procedure of determination of design strength M_d

Analogously, the design material strength M_d is to be calculated via characteristic strength values M_k at actual temperature, divided by resulting partial factors γ_m (Fig. 3). The characteristic strength values are defined as corresponding to specified fractiles of the probability density distribution. The different partial factors γ_m^1, γ_m^2, γ_m^3, and γ_m^4, are expressing the influence of the scatter in material strength, the uncertainty of the design model, the uncertainty in relation between material property in the structure and material property determined in test, and the safety class, respectively. The predicted extent of personal and property damage at failure - very serious, serious, not serious - decides the safety class.

A similar approach - as outlined for the design load effect S_d and the design mechanical strength M_d - can be applied also to the design fire load density q_d and the design thermal properties of the structural materials.

A methodology for a probabilistic analysis of fire exposed steel structures, connected to the described design method, has been developed in [8]. The methodology comprises a general systematized scheme for the identification and evaluation of the various sources and kinds of uncertainty in the differentiated structural fire engineering design. The structure of the methodology is quite general and applicable to a wide class of structures and structural elements.

Described in a more detailed way, a direct, differentiated, analytical design of fire exposed load-bearing structures or structural members, inside a fire compartment, includes the following steps - Fig. 4.

The basis of the design is given by the fully developed compartment fire exposure. Decisive entrance quantities then are

(1) nominal load and load factor for fire load density,
(2) combustion properties of this design fire load,
(3) size and geometry of the fire compartment,
(4) ventilation characteristics of the fire compartment, and
(5) thermal properties of structures enclosing the fire compartment.

These quantities jointly determine the rate of burning, the rate of heat release, and the design gas temperature-time curve of the complete fire process. Together with

(6) structural data for the proposed structure,
(7) thermal properties of structural materials, and
(8) coefficients of heat transfer for various surfaces of the structure

this design gas temperature-time curve gives the requisite information for a determination of the transient temperature fields of the fire exposed structure or structural members. With

(9) mechanical properties of structural materials (Fig. 3), and
(10) load characteristics

as further entrance quantities the time variation of restraint forces and moments, thermal stresses, and load-carrying capacity R can be determined. The lowest value of R during the complete fire process defines the design load-carrying capacity R_d.

Over nominal loads and load factors for dead load, live load, etc, statistically representative of a fire occasion, the design load effect at fire S_d is defined, interdependent on non-fire design procedure (Fig. 2).

A direct comparison between the design load-carrying capacity R_d and the design load effect at fire S_d decides whether the structure can fulfil its required function or not at a fire exposure.

For buildings containing activities, which are particularly important from, for instance, an economical point of view, there may be the motive for requiring that the building can be used again after a fire, almost immediately or very soon, for the current activities in a full extent. If a fire engineering design also includes such a requirement on re-serviceability of the structure after fire, the design procedure is to be as follows.

From the time curve of the load-carrying capacity R, the design residual load-carrying capacity R_{rd} of the structure after fire is obtained as an end information. This quantity R_{rd} must be compared with the design load effect at service, non-fire state, on the structure S_{rd}, given by the corresponding nominal loads and load factors for dead load, live load, etc.

For fire-exposed, exterior, load-bearing structures, the procedure for a direct, differentiated design will be modified. For such a structure,

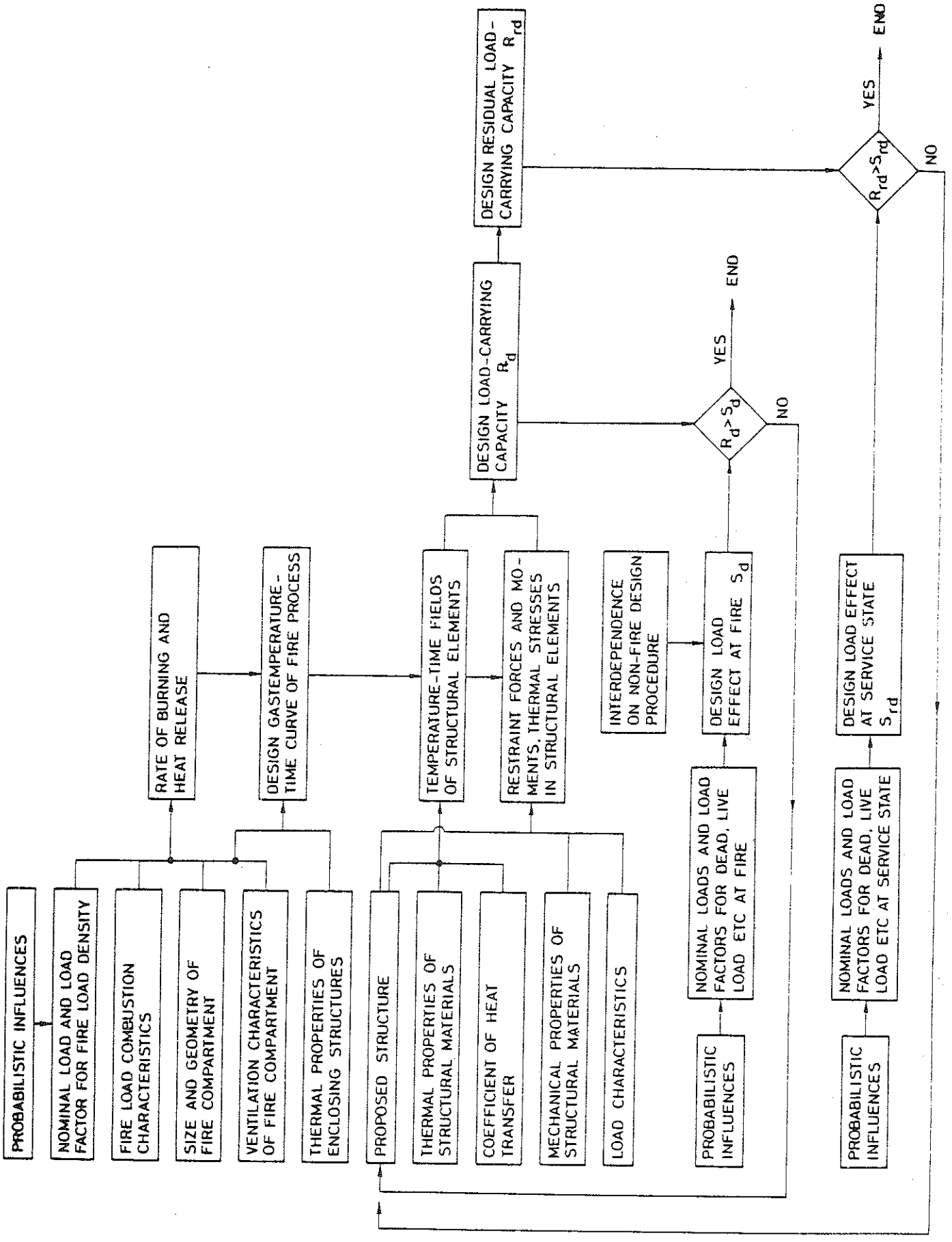

Figure 4. Procedure of a differentiated, analytical fire engineering design of load-bearing structures with additional requirement on re-serviceability after fire. Interior structures

the transient temperature fields are determined by a combined radiation and convection exposure from the flames and combustion gases outside the fire compartment as well as by radiation from the interior of the fire compartment through its window openings; cf., for instance [9], [10].

2. Fire Load Density and Gas Temperature-Time Curves of a Fully Developed Compartment Fire

At known combustion characteristics of the fire load, the gas temperature-time curve of a fully developed compartment fire can be calculated in the individual practical application from the heat and mass balance equations of the fire compartment with regard taken to the size, geometry and ventilation of the compartment, and to the thermal properties of the structures enclosing the compartment - Fig. 5 [2], [4], [6], [11], [12], [13], [14], [15], [16], [17].

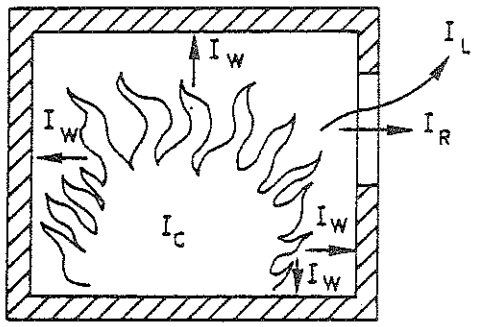

Figure 5. Energy balance equation $I_C = I_L + I_W + I_R$ of a fire compartment. I_C is the heat release per unit time from the combustion of the fuel, and I_L, I_W and I_R the quantities of energy removed per unit time by change of hot gases against cold air, by heat transfer to the surrounding structures, and by radiation through the openings of the compartment, respectively

For interior, load-bearing structures and partitions, the fire engineering design provisionally can be based on gas temperature-time curves T_t-t according to Fig. 6, [2], [4], [6], [13], which applies to a fire compartment with surrounding structures made of a material with a thermal conductivity $\lambda = 0.81\ W \cdot m^{-1} \cdot {}^oC^{-1}$ and a heat capacity $\rho c_p = 1.67\ MJ \cdot m^{-3} \cdot {}^oC^{-1}$ (fire compartment, type A). Entrance parameters of the diagrams are the fire load density q, defined by the formula

$$q = \frac{1}{A_t} \Sigma\, \mu_\nu m_\nu H_\nu \qquad (MJ \cdot m^{-2}) \qquad (1)$$

and the ventilation characteristics of the fire compartment, expressed by the opening factor $A\sqrt{h}/A_t$ ($m^{1/2}$), where

A = total area of window and door openings (m^2),
h = mean value of the heights of window and door openings, weighed with respect to each individual opening area (m),
A_t = total interior area of the surfaces bounding the compartment, opening areas included (m^2),
m_ν = total weight of combustible material ν (kg)
H_ν = effective heat value of combustible material ν of the fire load ($MJ \cdot kg^{-1}$), and
μ_ν = a fraction between 0 and 1, giving the real degree of combustion for each individual component of the fire load.

The non-dimensional factor μ_ν is a function of type of fuel, geometrical properties of fuel, and the position of fuel in a fire compartment, among other things. For some types of fire load components, μ_ν will depend on the time of fire duration and on the gas temperature-time characteristics of the fire compartment. Bookcases and floor coverings are examples of fire components whose real degree of combustion is low, and whose μ_ν values are probably appreciably below unity. At present, however, there is a lack of experimentally substantiated and verified μ_ν values, and it is therefore usually necessary in the course of practical design to employ a fire load calculation with μ_ν generally put equal to unity.

As a rule, the design fire load density is to be determined on the basis of statistical investigations for the type of building or premises in question. Such statistical investigations have been carried out for dwellings, offices, administration buildings, schools, stores, and hospitals [2], [4], [6]. As a temporary regulation, the Swedish Building Code authorizes the 80 percent level of the statistical distribution curve to be applied as the design fire load density.

The gas temperature-time curves in Fig. 6 have generally been determined on the assumption of ventilation controlled fires. For fires, which are fuel bed controlled in reality, this assumption leads to a structural fire engineering design on the safe side in practically every case, giving an overestimation of the maximum gastemperature and a simultaneous, partly

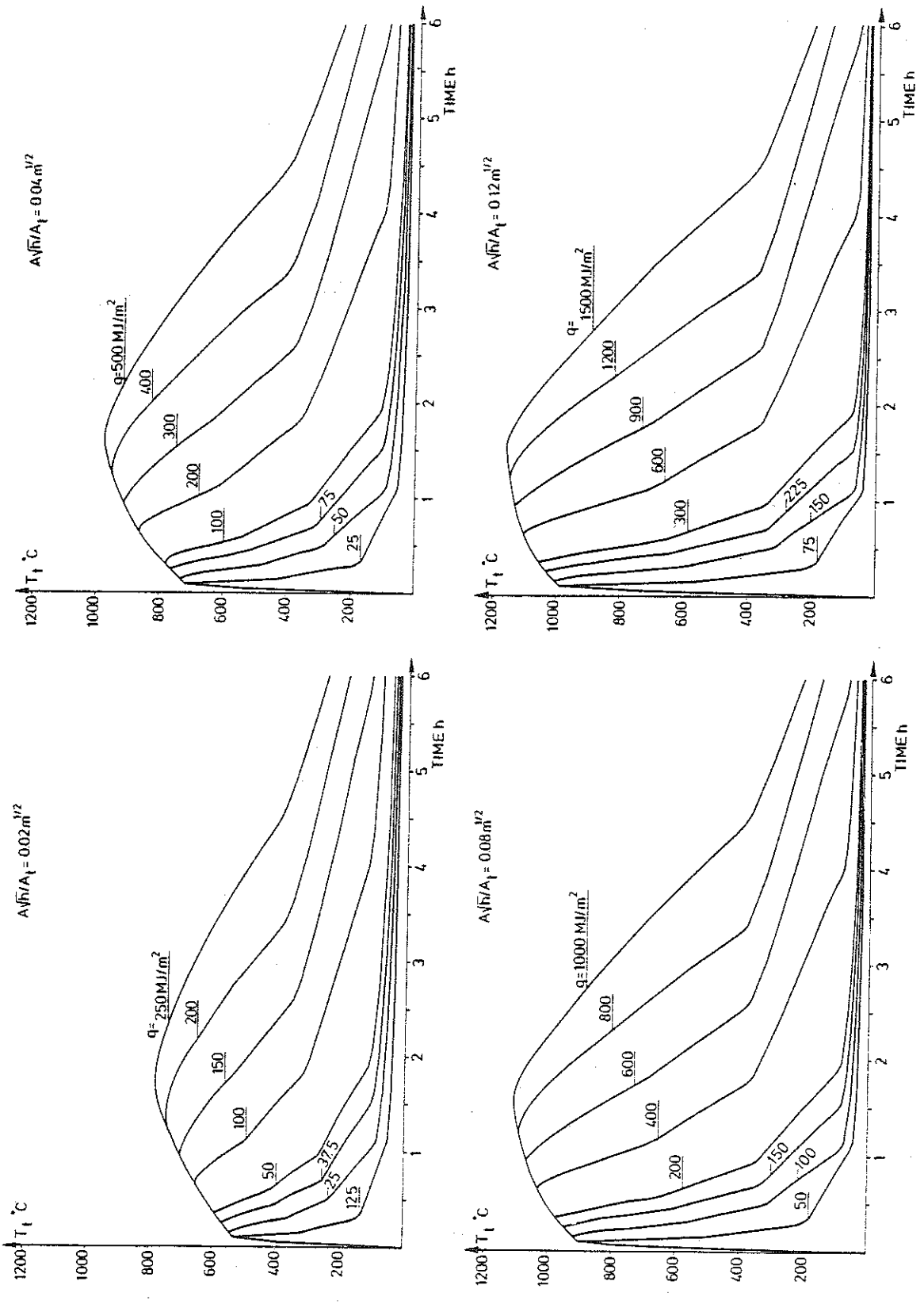

Figure 6. Gas temperature-time curves T_t-t of the complete process of fire development for different values of the fire load density q and the opening factor $A\sqrt{h}/A_t$. Fire compartment, type A

balancing underestimation of the fire duration. For the minimum load-bearing capacity, which thermally can be seen as an integrated effect, the gas temperature-time curves in Fig. 6 give reasonably correct results, verified in [4], [8], [14].

As pointed out, the gas temperature-time curves in Fig. 6 apply to a certain fire compartment, type A, specified with respect to the thermal properties of its surrounding structures. Fire compartments with surrounding structures of deviating thermal properties can be transferred to fire compartment, type A, via fictitious values of the fire load density q_f and the opening factor $(A\sqrt{h}/A_t)_f$ in accordance to Table 1 in the appendix [2], [4], [6].

3. Design Temperature State of Fire Exposed Steel Structures and Partitions

For a fire exposed, uninsulated steel structure, the energy balance equation gives the following formula for a determination of the steel temperature-time curve T_s-t - Fig. 7

$$\Delta T_s = \frac{\alpha}{\rho_s c_{ps}} \cdot \frac{F_s}{V_s} (T_t - T_s)\Delta t \qquad (^oC) \qquad (2)$$

where

ΔT_s = change of steel temperature (^oC) during time step Δt(s),
α = coefficient of heat transfer at fire exposed surface of structure ($W \cdot m^{-2} \cdot {}^oC^{-1}$),
ρ_s = density of steel material (7850 $kg \cdot m^{-3}$),
c_{ps} = specific heat of steel material ($J \cdot kg^{-1} \cdot {}^oC^{-1}$),
F_s = fire exposed surface of steel structure per unit length (m),
V_s = volume of steel structure per unit length (m^2),
T_t = gas temperature (^oC) within fire compartment at time t (s).

Eq. (2) presupposes that the steel temperature T_s is uniformly distributed over the cross section of the structure at any time t.

The coefficient of heat transfer α can be calculated from the approximate formula

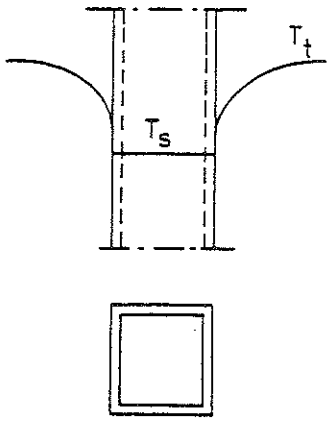

Figure 7. Fire exposed, uninsulated steel structure. T_t = gas temperature within fire compartment, T_s = steel temperature at time t

$$\alpha = 23 + \frac{5.77\ \varepsilon_r}{T_t - T_s}\left[\left(\frac{T_t + 273}{100}\right)^4 - \left(\frac{T_s + 273}{100}\right)^4\right] \quad (W \cdot m^{-2} \cdot {}^oC^{-1}) \quad (3)$$

giving an accuracy which is sufficient for ordinary practical purposes. ε_r is the resultant emissivity which for practical applications can be chosen according to the following table, giving values which generally are on the safe side.

1. Column, fire exposed on all sides	ε_r = 0.7
2. Column, outside a facade	0.3
3. Floor structure, composed of steel beams with a concrete slab on the lower flange of the beams	0.5
4. Steel beams with a floor slab on the upper flange of the beams	
4a. Beams of I cross section with width/height ≥ 0.5	0.5
4b. Beams of I cross section with width/height < 0.5	0.7
4c. Beams of box cross section and trusses	0.7

In [2], [4], [5], [6], more accurate values are given for the resultant emissivity ε_r, as concerns the application case 4.

At a given gas temperature-time curve T_t-t of the fire compartment, the steel temperature T_s can be directly calculated from Eqs. (2) and (3) with regard taken to the temperature dependence of c_{ps} and α. Such computations have been carried out in a systematized way, giving the basis of design in Table 2 [4]. From this table, the maximum steel temperature $T_{s,max}$ during a complete compartment fire can be determined directly as a function of the fictitious fire load density q_f, the fictitious opening

factor $(A\sqrt{h}/A_t)_f$, the F_s/V_s ratio and the resultant emissivity ε_r. The values of the table are connected to gas temperature characteristics according to Fig. 6.

For a fire exposed, insulated steel structure, analogously, a simplified energy balance equation gives the following formula for a direct determination of the steel temperature-time curve T_s-t - Fig. 8

$$\Delta T_s = \frac{A_i}{(1/\alpha + d_i/\lambda_i)\rho_s c_{ps} V_s} (T_t - T_s)\Delta t \qquad (^oC) \qquad (4)$$

with the additional quantities

A_i = interior jacket surface area of insulation per unit length (m),
d_i = thickness of insulation (m),
λ_i = thermal conductivity of insulating material ($W \cdot m^{-1} \cdot {}^oC^{-1}$).

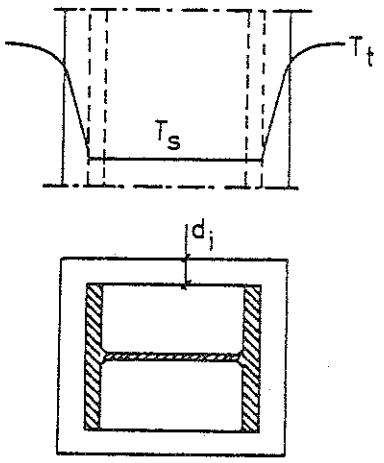

Figure 8. Fire exposed, insulated steel structure. T_t = gas temperature within fire compartment, T_s = steel temperature at time t

Eq. (4) presupposes that the steel temperature T_s is uniformly distributed over the cross section of the structure at any time t, that the temperature gradient is linear and the heating contribution negligible for the insulation, and that the heat transfer is one-dimensional.

Computations, originating from Eqs. (3) and (4), enable a production of a systematized design basis, facilitating an analytical, differentiated fire engineering design in practice. An example from such a design basis is referred in Table 3 [4], giving the maximum steel temperature $T_{s,max}$ during a complete compartment fire for varying values of the fictitious fire load density q_f, the fictitious opening factor $(A\sqrt{h}/A_t)_f$, the structural parameter A_i/V_s, and the insulation parameter d_i/λ_i. The values of the table are connected to gas temperature characteristics according to Fig. 6.

Table 3 has been computed on the assumption of a constant thermal conductivity of the insulating material λ_i, chosen as an average value for the whole compartment fire process. Calculations, carried through systematically, are verifying that this average value of λ_i approximately coincides with the value, determined for an insulation temperature equal to the maximum steel temperature $T_{s,max}$.

For a specific insulating material, systematized design diagrams or tables can be computed very accurately with regard to the temperature dependence of the thermal properties of the steel as well as the insulating material. The influence of an initial moisture content and of a disintegration of the insulating material can be considered, too. Practically, such a determination can be carried out over a numerical data processing by computers on the basis of a finite difference or a finite element method. A great number of design tables, computed according to such an accurate procedure, are presented in [4]. Table 4 exemplifies this, giving the maximum steel temperature $T_{s,max}$ at varying fire and structural design characteristics for a fire exposed steel structure, insulated with gypsum plaster slabs, type Gyproc, of density 790 $kg \cdot m^{-3}$. The thermal properties of the gypsum plaster slabs then have been assumed to depend on the insulation temperature according to Fig. 9 [18], constructed on the basis of results from small scale and full scale tests and of information in the literature [19]. The influence of the disintegration of the slab material is considered.

In [4], an analytical model is derived for a simplified determination of the temperature-time fields of a steel beam construction according to Fig. 10 - composed of a reinforced concrete slab, load-bearing steel beams, and an insulating ceiling - exposed to a fire from below. By applying this computational model in a systematic way, a design basis has been determined, facilitating a calculation of the steel beam temperature T_s, assumed as uniformly distributed over the cross section of the beams. The design basis is exemplified in Table 5 [4], which gives the maximum steel beam temperature $T_{s,max}$ during a complete compartment fire for varying values of the fictitious fire load density q_f, the fictitious opening factor $(A\sqrt{h}/A_t)_f$, the structural parameter F_s/V_s, and the insulation parameter d_i/λ_i. F_s denotes the surface area of the steel beam, less the part covered by the concrete slab, and V_s the volume of the steel beam, per unit length. The

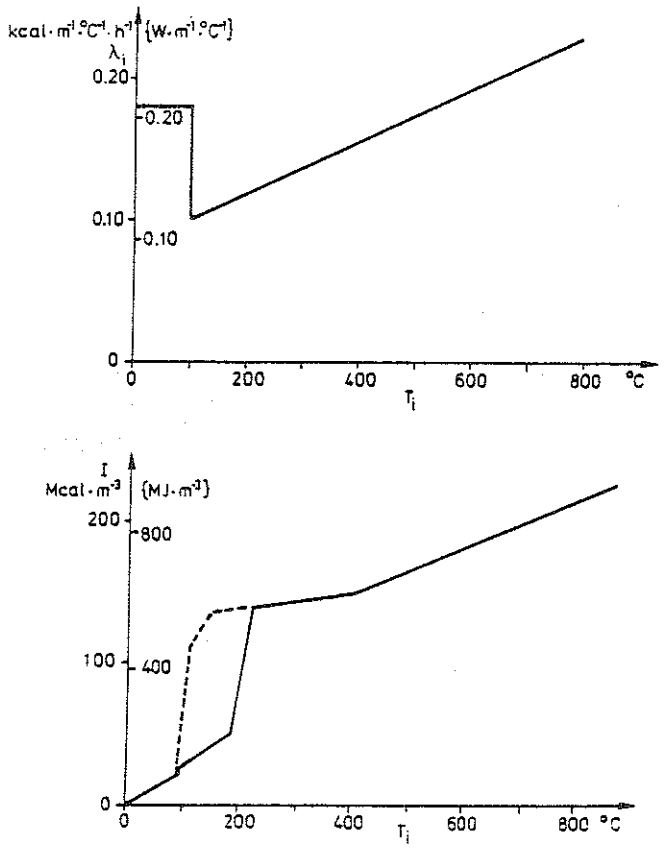

Figure 9. Thermal conductivity λ_i and enthalpy I ($= \int_0^T c_p dT$) as a function of insulation temperature T_i for gypsum plaster slabs, type Gyproc, of density 790 kg·m^{-3}. For enthalpy I, full line refers to a rapid heating and dashed line to a slow heating [18]

values, given in brackets in the table, denote the corresponding maximum temperature at the centre level of the ceiling. The values of the table are connected to gas temperature characteristics according to Fig. 6.

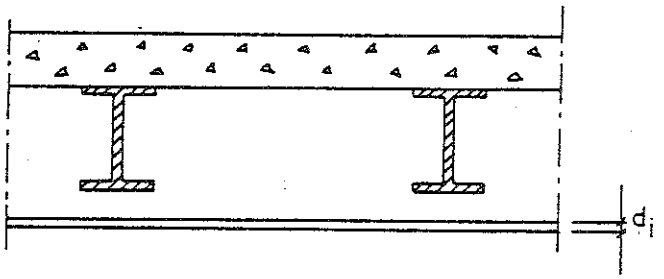

Figure 10. Floor structure, composed of a reinforced concrete slab, load-bearing steel beams, and an insulating ceiling

For several types of steel beam constructions with a suspended, insulating ceiling, the fire resistance of the ceiling and its fastening devices will be the decisive design criterion instead of the temperature of the steel beams. The ceiling can get a serious crack formation or fall down, partially or completely, after a comparatively short fire exposure. Under such conditions, the maximum steel beam temperature cannot be determined from Table 5 solely on the basis of the thickness d_i and the thermal conductivity λ_i of the ceiling. If results are available for a type of a suspended ceiling from a standard fire resistance test, these results can be used for deriving a fictitious value of the insulation parameter d_i/λ_i - $(d_i/\lambda_i)_{fict}$ - which describes the real fire behaviour of the suspended ceiling, including its fastening devices. From the test results, also a possible critical failure temperature of the suspended ceiling can be estimated. Cf., further [4].

After the determination of $(d_i/\lambda_i)_{fict}$ and the critical temperature of a type of a suspended ceiling, the analytical differentiated fire design can be carried out by a direct application of Table 5. Parallelly, then the maximum temperature at the centre level of the ceiling according to the table must be controlled against the critical temperature of the ceiling.

Fictitious d_i/λ_i values and critical temperatures have been determined for a number of types of suspended ceilings in a series of standard fire resistance tests performed at the National Swedish Institute for Testing and Metrology in Stockholm [20]. The compositions of these suspended ceilings, the results obtained and the characteristics derived are set out in Table 6 [4].

The design basis, reproduced in Table 2 to 5, generally assumes the steel temperature to be uniformly distributed over the cross section of the beam or column at any time t. A more accurate theory, which enables a determination of the temperature variation over the cross section of the steel structure, is presented in [21], together with computer routines. The algorithm described can easily be coupled to most finite element programs. An illustration of the capability of the theory is given in Fig. 11, which shows calculated temperature distribution along the line of symmetry of a gypsum insulated steel beam with a concrete slab at the top flange at selected times of a standard fire resistance test according to ISO 834.

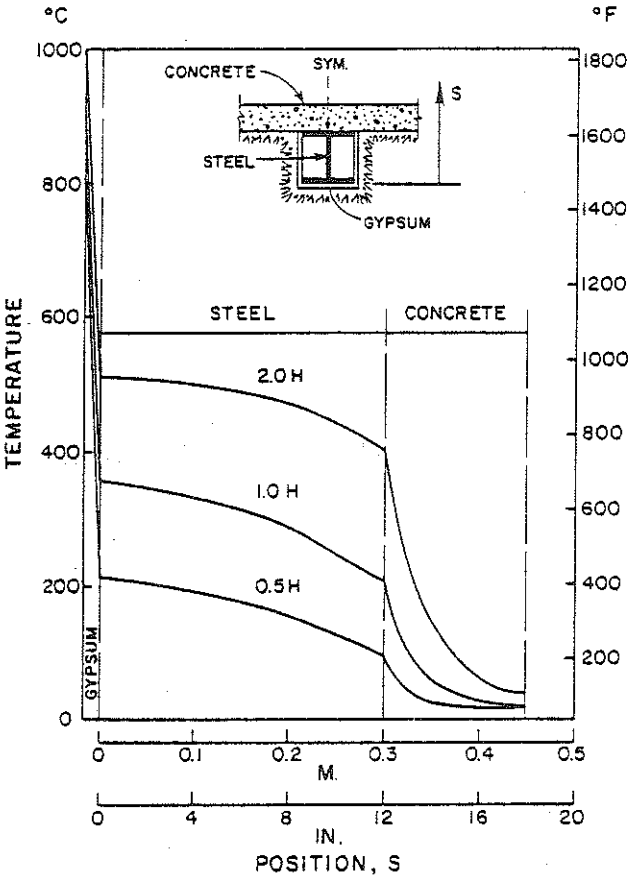

Figure 11. Calculated temperature distribution along line of symmetry of a steel beam, insulated by a 16 mm gypsum board (density 770 kg·m^{-3}) and carrying a 150 mm concrete slab on top flange, at selected times of a thermal exposure according to ISO 834 [21]

As a complement to the design temperature state of fire exposed load-bearing steel structures, dealt with above, also some remarks will be given on the fire engineering design of partitions. The performance requirements for partitions imply that these must prevent a penetration of flames and hot gases and limit the rise in temperature on the unexposed side of the construction during a complete compartment fire.

An analytical method for a determination of the temperature-time field in a multi-layer partition is presented in [18]; cf. also [4]. The method considers the temperature dependence of the thermal material properties, an initial moisture content, and a possible material disintegration at specified temperature criteria. An illustrating application of the method is shown in Fig. 12 [18], which gives a summary conception

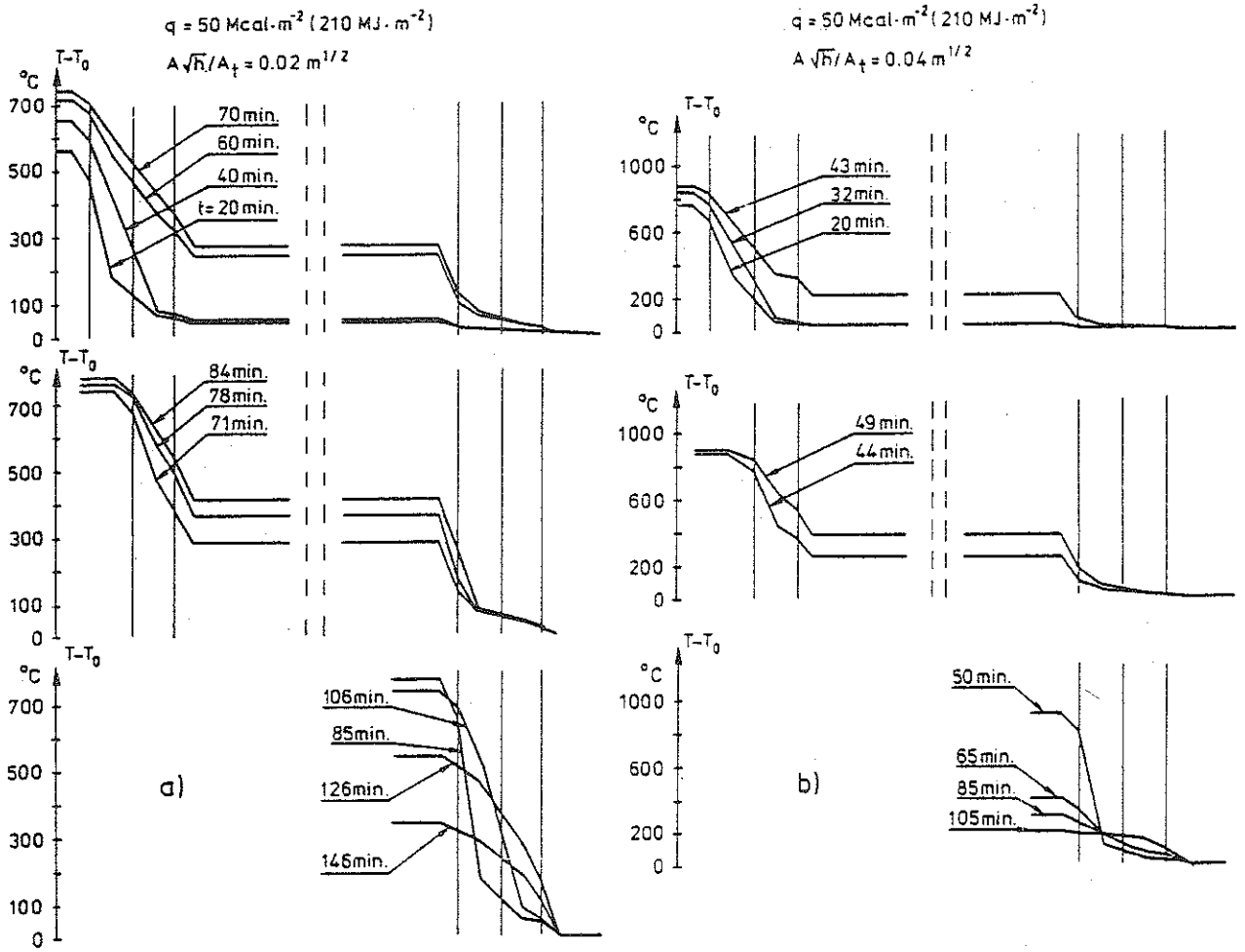

Figure 12. Calculated temperature-time fields for a steel stud wall, insulated on each side with two 13 mm gypsum plaster sheets, type Gyproc, of density 790 kg·m^{-3}. The wall is fire exposed on one side with compartment fire characteristics according to Fig. 6: a) q = 50 Mcal·m^{-2} (210 MJ·m^{-2}), $A\sqrt{h}/A_t$ = 0.02 m$^{1/2}$; b) q = 50 Mcal·m^{-2} (210 MJ·m^{-2}), $A\sqrt{h}/A_t$ = 0.04 m$^{1/2}$. T_o = temperature at time t = 0 [18]

of the fire behaviour of a steel stud wall, insulated on each side with two 13 mm gypsum plaster sheets, type Gyproc, of density 790 kg·m^{-3}, fire exposed on one side and acting as a partition. The behaviour has been determined on the basis of temperature dependent thermal properties of gypsum plaster material according to Fig. 9 and a critical failure temperature for a gypsum plaster sheet of 550°C on that side of the sheet facing away from the fire. The results of full scale fire tests confirm this failure criterion.

Fig. 12a describes the fire behaviour of the wall, when it is fire exposed on one side by a compartment fire with gas temperature-time

characteristics according to Fig. 6 - fire load density q = 50 Mcal·m^{-2} (210 MJ·m^{-2}), opening factor $A\sqrt{h}/A_t$ = 0.02 m$^{1/2}$. The figure gives a calculated failure of the directly fire exposed gypsum plaster sheet after about 70 min and of the next gypsum plaster sheet after about 85 min. The maximum temperature rise on the unexposed side of the wall amounts to 180°C during the complete fire process, i.e. precisely the maximum permissible value according to [2]. Fig. 12b analogously describes the fire behaviour of the wall, when it is exposed to a more rapid compartment fire - opening factor $A\sqrt{h}/A_t$ = 0.04 m$^{1/2}$ - at the same fire load density q. The increase of the opening factor results in a considerably decreased value of the maximum temperature rise on the unexposed side of the wall, which amounts to only about 55°C in this case.

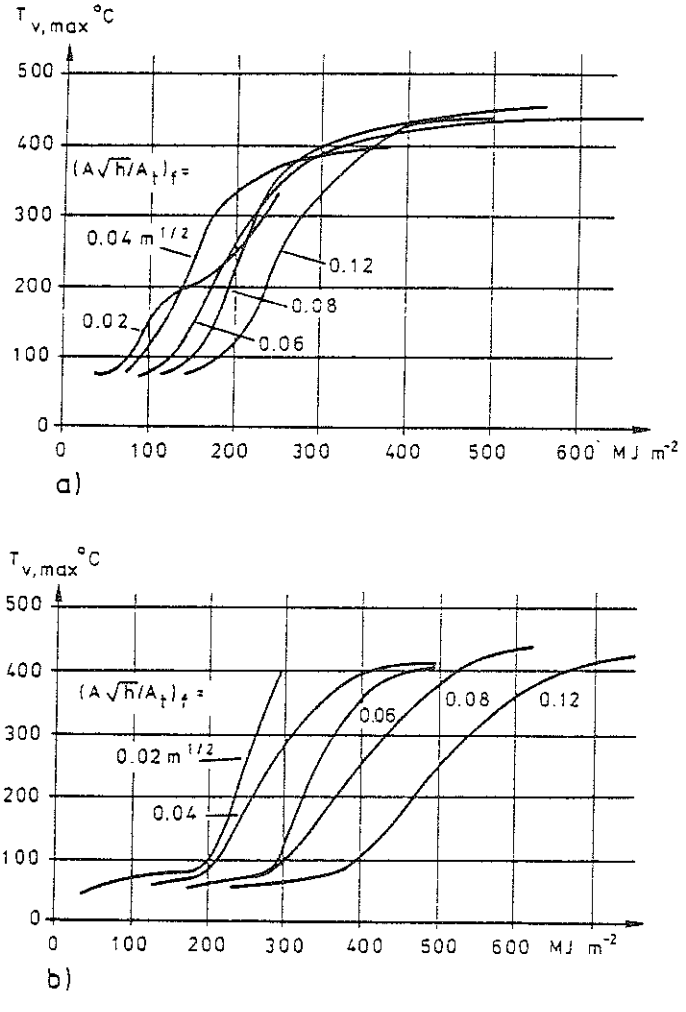

Figure 13. Maximum temperature $T_{v,max}$ during a complete fire process according to Fig. 6 on the unexposed side of a steel-gypsum plaster sheeting wall as a function of the fictitious fire load density q_f and the fictitious opening factor $(A\sqrt{h}/A_t)_f$ of the fire compartment. The wall is insulated on each side with one (fig a) or two (fig b) 13 mm gypsum plaster sheets, type Gyproc, of density 790 kg·m^{-3} [4], [6]

Systematic calculations of the type, illustrated by Fig. 12, lead to design diagrams as shown in Fig. 13 [4], [6], giving the maximum temperature $T_{v,max}$ during a complete fire process on the unexposed side of a steel stud-gypsum plaster sheeting wall as a function of the fictitious fire load density q_f and the fictitious opening factor of the fire compartment $(A\sqrt{h}/A_t)_f$. The two diagrams apply to an insulation on each side of the wall with one and two 13 mm gypsum plaster sheets, type Gyproc, of density 790 $kg \cdot m^{-3}$, respectively. The calculated $T_{v,max}$ values are to be compared with the corresponding maximum temperature, permitted in the Swedish Building Code, which implies 200°C as an average temperature and 240°C as a temperature over limited areas of the unexposed side of the partition [2].

4. Design Load-Bearing Capacity of Fire Exposed Steel Structures

By applying the design tables 2 to 5, the maximum steel temperature $T_{s,max}$ can be determined comparatively quickly for an uninsulated or insulated steel structure, exposed to a complete compartment fire with gas temperature-time characteristics according to Fig. 6. The corresponding design load-bearing capacity of the structure then is obtained by design diagrams of the type exemplified in Fig. 14, 15 and 16.

Fig. 14 and 15 [4], [6] give the design load-bearing capacity (M_{cr}, P_{cr}, q_{cr}) of fire exposed beams of constant I cross section at different types of loading and support conditions, as a function of the steel beam temperature T_s. The design curves in Fig. 14 apply to a slow rate of heating - assumed to be 4 $^{o}C \cdot min^{-1}$, followed by a cooling with a rate of 1.33 $^{o}C \cdot min^{-1}$ - and Fig. 15 gives the correction $\Delta\beta$ of the load-bearing capacity coefficient β due to a more rapid rate of heating. In the formulas for the load-bearing capacity

σ_s = yield stress of steel material at room temperature (MPa),
L = span of beam (m),
W = elastic modulus of beam cross section (m^3).

The design curves in Fig. 14 and 15 have been determined on the basis of the deformation curve of the fire exposed beams calculated by an

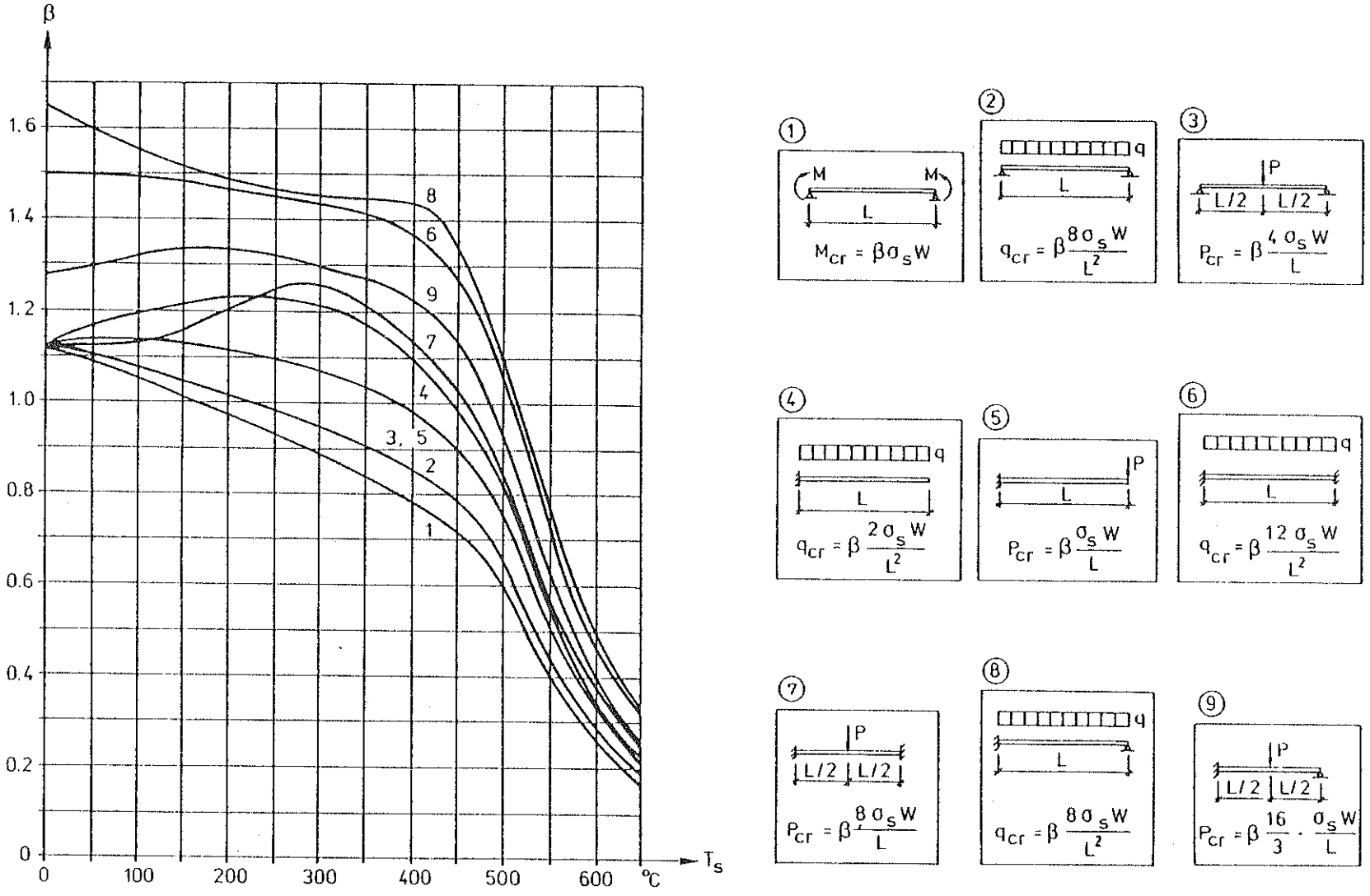

Figure 14. Coefficient β for determination of critical load (M_{cr}, P_{cr}, q_{cr}) for fire exposed beams of I cross section at different types of loading and support conditions, as a function of the steel beam temperature T_s. The curves have been calculated for a slow rate of heating of 4 $^{o}C \cdot min^{-1}$ and a subsequent cooling, assumed to be one third of the rate of heating [4], [6]

analytical model, presented in [22], which takes into account the softly rounded shape of the stress-strain curve of steel at elevated temperatures as well as the influence of creep strain. As can be seen from Fig. 15, this influence of creep begins to be noticeable for ordinary structural steels at temperatures in excess of about 450°C. The load-bearing capacity of the beams is defined by the limit deflection criterion according to ROBERTSON and RYAN [23].

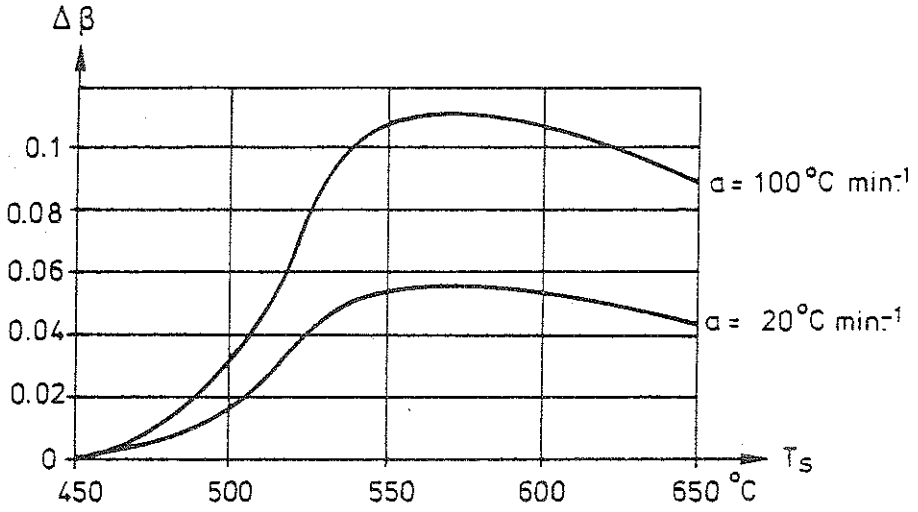

Figure 15. Increase $\Delta\beta$ of coefficient β, determined according to Fig. 14, for a rate of heating $a \geq 4\ ^{o}C \cdot min^{-1}$, as a function of the steel beam temperature T_s [4], [6]

The diagrams in Fig. 16 [4] determine the variation with the steel temperature T_s of the relationship between the buckling stress σ_{cr} and the slenderness ratio λ for fire exposed columns, axially loaded in compression. The diagrams apply to steel having a yield stress at room temperature σ_s = 220, 260 and 320 MPa, respectively, and are valid under the presumption that the column is unrestrained with respect to longitudinal expansion during the fire exposure. The σ_{cr}-λ curves have been computed for an initially deflected and excentrically loaded column on the basis of data on the change of the 0.5 % proof stress $\sigma_{0.5}$ and the secant modulus with the temperature, obtained in tension tests at a very slow rate of loading. This implies that a considerable influence of short-time creep at elevated temperatures is included.

For a fire engineering design of columns, partly restrained to a longitudinal expansion, reference is made to [4].

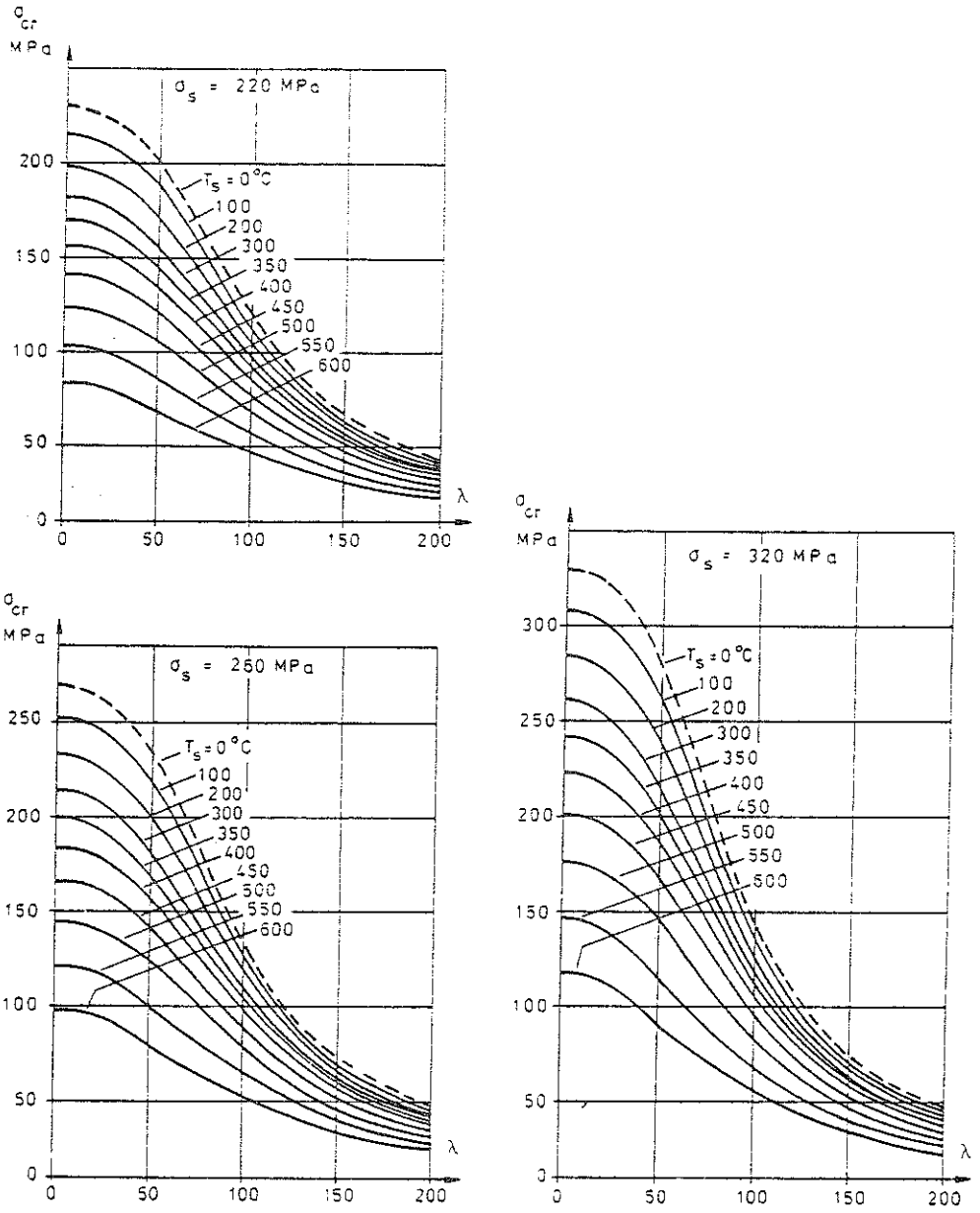

Figure 16. Variation with steel temperature T_s of the relationship between buckling stress σ_{cr} and slenderness ratio λ for fire exposed steel columns, axially loaded in compression, free to expand longitudinally and made of steel having a yield stress at room temperature σ_s = 220, 260 and 320 MPa, respectively [4], [6]

The design curves, reproduced in Fig. 14, 15 and 16, are generally based on the assumption of a uniformly distributed temperature over the cross section of the steel structure at any time t during the fire exposure. By this assumption, the design curves are directly connected to Tables 2 to 5, determining the design temperature state of the steel structure.

If the analytical, differentiated design of fire exposed steel structures will be further developed in future towards a more accurate determination

of the design temperature state, with regard taken to the temperature variation over the cross section of the steel structure, this will also require a more refined basis of design for the transfer of the design temperature state to the design load-bearing capacity of the fire exposed structure. The first attempts of developing such a more refined design basis now can be noticed in the literature. As a fragmentary example of this development, Fig. 17 [24] shows the calculated variation of the plastic bending moment of a fire exposed steel I cross section as a function of the maximum temperature for various linear temperature distributions over the cross section.

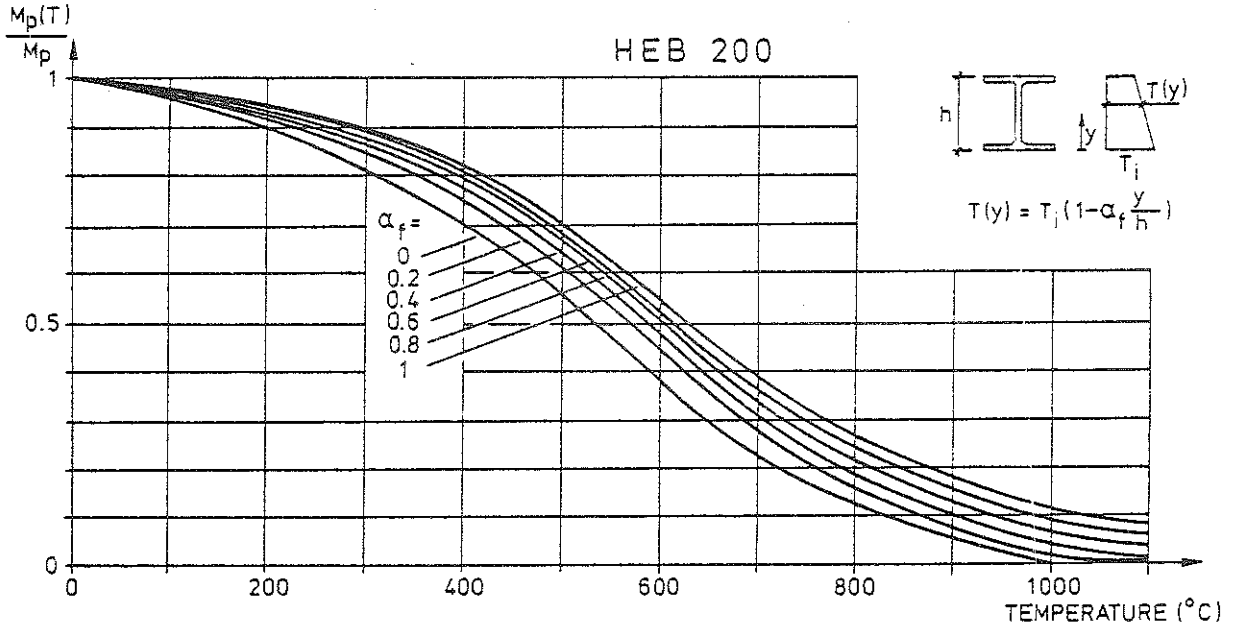

Figure 17. Calculated variation of plastic bending moment $M_p(T)$ in terms of various linear temperature distribution over height of a steel I cross section [24]

5. Summary

A differentiated procedure is presented for an analytical fire engineering design of load-bearing steel structures and partitions. The procedure is a direct design method based on gas temperature-time characteristics of a complete compartment fire, which depend on the fire load density, the ventilation of the fire compartment and the thermal properties of the structures enclosing the fire compartment. The practical use of the deisgn procedure has been approved by the National Swedish Board of Physical Planning and Building.

For the practical application of the design procedure, a comprehensive design basis in the form of diagrams and tables has been worked out for a direct determination of the maximum steel temperature during a complete compartment fire and the corresponding design load-bearing capacity of the fire exposed structure. This design basis is exemplified in the paper, focused to steel structures with an insulation of gypsum plaster slabs, primarily for giving a rough impression of the character of the analytical design procedure.

Compared with the conventional fire engineering design, based on classification and results of standard fire resistance tests, the presented analytical design procedure has a more logical structure, based on well-defined functional requirements and performance criteria, gives a structural fire design with a better economy, and leads to a more consistent fire safety level.

References

[1] MAGNUSSON, S.E. and PETTERSSON, O.: Functional Approaches - An Outline. Final Report, CIB W14 Symposium "Fire Safety in Buildings: Needs and Criteria", held in Amsterdam 1977-06-02/03, p. 120-145.

[2] NATIONAL SWEDISH BOARD OF PHYSICAL PLANNING AND BUILDING: Brandteknisk dimensionering (Fire Engineering Design). Comments on SBN (Swedish Building Code), No. 1976:1.

[3] PETTERSSON, O.: Principles of Fire Engineering Design and Fire Safety of Tall Buildings. ASCE-IABSE International Conference on Planning and Design of Tall Buildings, Lehigh University, Bethlehem, Pa., August 21-26, 1972, Summary Report of Technical Committee 8, Conference Preprints, Vol. DS. - Bulletin 31, Division of Structural Mechanics and Concrete Construction, Lund Institute of Technology, Lund, 1973.

[4] PETTERSSON, O., MAGNUSSON, S.E. and THOR, J.: Fire Engineering Design of Steel Structures. Swedish Institute of Steel Construction, Publication No. 50, Stockholm 1976 (Swedish edition 1974).

[5] PETTERSSON, O.: Calcul Théoretique des Structures Exposées au Feu,

Sécurite de la Construction Face à L'Incendie, Séminaire tenu à Saint-Rémy-lès Chevreuse (France) du 18 au 20 Novembre 1975, Editions Eyrolles, Paris, 1977, pp. 175-224. - Theoretical Design of Fire Exposed Structures. Bulletin 51, Division of Structural Mechanics and Concrete Construction, Lund Institute of Technology, Lund, 1976.

[6] PETTERSSON, O. and ÖDEEN, K.: Brandteknisk dimensionering av byggnadskonstruktioner - principer, underlag, exempel (Fire Engineering Design of Building Structures - Principles, Design Basis, Examples). Liber Förlag, Stockholm, 1978.

[7] NATIONAL SWEDISH BOARD OF PHYSICAL PLANNING AND BUILDING, Safety Group: Allmänna bestämmelser för bärande konstruktioner, AK 77, del 1. Säkerhetsbestämmelser (General Regulations for Load-Bearing Structures, AK 77, Part 1, Safety Regulations). Draft Proposal, Stockholm, 1976-11-24.

[8] MAGNUSSON, S.E.: Probabilistic Analysis of Fire Exposed Steel Structures. Bulletin 27, Division of Structural Mechanics and Concrete Construction, Lund Institute of Technology, Lund, 1974.

[9] LAW, M.: Design Guide for Fire Safety of Bare Exterior Structural Steel. 1. Theory and Validation. 2. State of the Art. Ove Arup & Partners. London, January 1977.

[10] BECHTOLD, R.: Zur thermischen Beanspruchung von Aussenstützen im Brandfall. Heft 37, Institut für Baustoffkunde und Stahlbetonbau, Technische Universität, Braunschweig, September 1977.

[11] KAWAGOE, K. and SEKINE, T.: Estimation of Fire Temperature-Time Curve in Rooms. Occasional Report No. 11, Building Research Institute, Tokyo, 1963. - KAWAGOE, K.: Estimation of Fire Temperature-Time Curve in Rooms. Research Paper No. 29, Building Research Institute, Tokyo, 1967.

[12] ÖDEEN, K.: Theoretical Study of Fire Characteristics in Enclosed Spaces. Bulletin 19, Division of Building Construction, Royal Institute of Technology, Stockholm, 1963.

[13] MAGNUSSON, S.E. and THELANDERSSON, S.: Temperature-Time Curves for the Complete Process of Fire Development. A Theoretical Study of Wood Fuel Fires in Enclosed Spaces. Acta Polytechnica Scandinavica, Ci 65, Stockholm, 1970.

[14] MAGNUSSON, S.E. and THELANDERSSON, S.: A Discussion of Compartment Fires. Fire Technology, Vol. 10, No. 3, August 1974.

[15] HARMATHY, T.Z.: A New Look at Compartment Fires. Part I, Fire Technology, Vol. 8, No. 3, August 1972, and Part II, Fire Technology, Vol. 8, No. 4, November 1972.

[16] BABRAUSKAS, V. and WILLIAMSON, R.B.: Post-Flashover Compartment Fires. University of California, Berkeley, Fire Research Group, Report No. UCB FRG 75-1, December 1975. - Post-Flashover Compartment Fires: Basis of a Theoretical Model. Fire and Materials, Vol. 2, No. 2, April 1978.

[17] THOMAS, P.H.: Some Problem Aspects of Fully Developed Room Fires. Symposium on "Fire Standards and Safety", Washington, 5-6 April 1976.

[18] MAGNUSSON, S.E. and PETTERSSON, O.: Brandteknisk dimensionering av isolerad stålkonstruktion i bärande eller avskiljande funktion (Fire Engineering Design of Insulated Load-Bearing or Separating Steel Structures). Väg- och vattenbyggaren No. 4, Stockholm, 1969.

[19] HARMATHY, T.Z.: A Treatise on Theoretical Fire Endurance Rating. Research Paper No. 153, Division of Building Research, National Research Council, Canada, Ottawa, 1962.

[20] ÖDEEN, K. and ANÄS, B.: Brandskyddande undertak för stålkonstruktioner (Fire Protection for Steel Structures in the Form of a Suspended Ceiling). Byggmästaren No. 12, Stockholm, 1969.

[21] WICKSTRÖM, U.: A Numerical Procedure for Calculating Temperature in Hollow Structures Exposed to Fire. Fire Research Group, University of California, Report No. UCB FRG 77-9, Berkeley, August 1977.

[22] THOR, J.: Deformations and Critical Loads of Steel Beams Under Fire Exposure Conditions. National Swedish Building Research, Document D16:1973, Stockholm.

[23] ROBERTSON, A.F. and RYAN, I.V.: Proposed Criteria for Defining Load Failure of Beams, Floors and Roof Constructions during Fire Tests. Journal of Research, National Bureau of Standards, Vol. 63 C, Washington, 1959.

[24] KRUPPA, J.: Résistance au Feu des Structures Métalliques en Température Non Homogène. Thèse, Présentée devant l'Institut National des Sciences Appliquées de Rennes pour l'obtention du grade de Docteur-Ingenieur en Genie Civil, 27 Juin 1977.

Acknowledgement

This paper is mainly based on results, published in different connections, from the research activities within the fire research group at the Division of Structural Mechanics and Concrete Construction, Civil Engineering Department, Lund University. In substantial extent, this fire research is financially sponsored by the National Swedish Council for Building Research, Stockholm.

APPENDIX

Table 1. Coefficient K_f for transforming a real fire load density q and a real opening factor of a fire compartment $A\sqrt{h}/A_t$ to a fictitious fire load density q_f and a fictitious opening factor $(A\sqrt{h}/A_t)_f$ corresponding to a fire compartment, type A

$$q_f = K_f \, q \qquad (A\sqrt{h}/A_t)_f = K_f \, A\sqrt{h}/A_t$$

Type of fire compartment	Opening factor $A\sqrt{h}/A_t$ $m^{1/2}$					
	0.02	0.04	0.06	0.08	0.10	0.12
Type A	1	1	1	1	1	1
Type B	0.85	0.85	0.85	0.85	0.85	0.85
Type C	3.00	3.00	3.00	3.00	3.00	2.50
Type D	1.35	1.35	1.35	1.50	1.55	1.65
Type E	1.65	1.50	1.35	1.50	1.75	2.00
Type F[1)]	1.00-0.50	1.00-0.50	0.80-0.50	0.70-0.50	0.70-0.50	0.70-0.50
Type G	1.50	1.45	1.35	1.25	1.15	1.05

[1)] The lowest value of K_f applies to a fire load density $q > 500$ MJ·m^{-2}, the highest value to a fire load density $q \leq 60$ MJ·m^{-2}. For intermediate fire load densities, linear interpolation gives sufficient accuracy.

The different types of fire compartment are defined as follows

Fire compartment, type B: Bounding structures of concrete.

Fire compartment, type C: Bounding structures of lightweight concrete (density $\rho = 500$ kg·m^{-3}).

Fire compartment, type D: 50% of the bounding structures of concrete, and 50% lightweight concrete (density $\rho = 500$ kg·m^{-3}).

Fire compartment, type E: Bounding structures with the following percentage of bounding surface area:
50% lightweight concrete (density $\rho = 500$ kg.m^{-3}),
33% concrete,
17% of from the interior to the exterior: plasterboard panel (density $\rho = 790$ kg·m^{-3}), 13 mm in thickness - diabase wool (density $\rho = 50$ kg·m^{-3}), 10 cm in thickness - brickwork (density $\rho = 1800$ kg·m^{-3}), 20 cm in thickness.

Fire compartment, type F: 80% of the bounding structures of sheet steel, and 20% of concrete. The compartment corresponds to a storage space with a sheet steel roof, sheet steel walls, and a concrete floor.

Fire compartment, type G: Bounding structures with the following percentage of bounding surface area:
20% concrete,
80% of from the interior to the exterior: double plasterboard panel (density ρ=790 kg·m^{-3}), 2x13 mm in thickness - air space, 10 cm in thickness - double plasterboard panel (density ρ = 790 kg·m^{-3}), 2x13 mm in thickness.

For fire compartments, not directly represented in the table, the coefficient K_f can either be determined by a linear interpolation between applicable types of fire compartment in the table or be chosen in such a way as to give results on the safe side. For fire compartments with surrounding structures of both concrete and lightweight concrete, then different values can be obtained of the coefficient K_f, depending on the choice between the fire compartment types B, C, and D at the interpolation. This is due to the fact that the relationships, determining K_f, are non-linear. However, the K_f-values of the table are such that a linear interpolation always gives results on the safe side, irrespective of the alternative of interpolation chosen. In order to avoid an unnecessarily large overestimation of K_f, that alternative of interpolation is recommended which gives the lowest value of K_f.

Table 2. Maximum steel temperature $T_{s,max}$ (°C) for uninsulated steel structure as a function of fictitious fire load density q (Mcal·m^{-2}) {MJ·m^{-2}}, fictitious opening factor $A\sqrt{h}/A_t$ ($m^{1/2}$), F_s/V_s ratio (m^{-1}), and resultant emissivity ε_r [4]

q	$A\sqrt{h}/A_t$	F_s/V_s	$T_{s,max}$ ε_r 0.3	ε_r 0.5	ε_r 0.7
10 {42}	0,01	50	325	345	370
		75	365	385	405
		100	395	410	425
		125	410	425	435
		150	425	435	440
		200	435	445	445
		400	450	450	450
	0,02	50	335	380	410
		75	410	445	475
		100	445	490	520
		125	480	520	545
		150	500	540	565
		200	540	560	575
		400	575	585	585
	0,04	50	285	320	365
		75	350	400	450
		100	405	460	510
		125	450	515	555
		150	495	555	595
		200	550	605	645
		300	625	660	690
	0,06	50	235	275	330
		75	305	370	425
		100	365	410	455
		125	415	450	545
		150	450	485	580
		200	520	550	660
		300	615	680	735
	0,08	50	200	250	300
		75	270	330	400
		100	330	400	460
		125	380	450	510
		150	410	510	580
		200	480	590	660
		300	600	700	780
	0,12	50	170	200	205
		75	220	260	350
		100	240	310	400
		125	260	380	540
		150	310	430	620
		200	380	500	700
		300	450	620	800
12,5 {52,5}	0,01	50	365	385	405
		75	410	425	435
		100	430	445	450
		125	440	450	460
		150	450	455	460
		200	455	460	465
		400	465	470	470
	0,02	50	380	435	470
		75	455	500	535
		100	500	540	560
		125	525	555	575
		150	550	570	580
		200	570	590	600
		400	600	605	605
	0,04	50	340	400	450
		75	415	485	540
		100	485	550	600
		125	535	600	640
		150	570	625	665
		200	630	665	700
	0,06	50	290	335	400
		75	365	425	495
		100	425	480	560
		125	480	525	610
		150	520	560	630
		200	580	625	705
		300	670	740	770
	0,08	50	250	315	360
		75	325	400	455
		100	385	475	535
		125	435	530	600
		150	485	585	650
		200	550	660	730
		300	655	770	-
	0,12	50	200	250	330
		75	240	320	410
		100	280	400	510
		125	340	450	620
		150	380	510	690
		200	500	600	760
		300	600	720	-

q	$A\sqrt{h}/A_t$	F_s/V_s	$T_{s,max}$ ε_r 0.3	ε_r 0.5	ε_r 0.7
15 {63}	0,01	50	400	420	440
		75	435	445	460
		100	450	460	470
		125	460	470	475
		150	470	475	480
		200	475	480	480
		400	480	485	485
	0,02	50	425	480	515
		75	500	540	565
		100	540	575	595
		125	565	600	610
		150	585	605	615
		200	605	620	625
		400	625	630	630
	0,04	50	400	455	510
		75	490	550	600
		100	550	610	655
		125	600	655	690
		150	635	680	710
	0,06	50	340	400	475
		75	425	490	575
		100	500	550	630
		125	550	600	680
		150	590	630	720
		200	650	700	755
	0,08	50	300	375	430
		75	380	465	535
		100	450	545	605
		125	500	595	670
		150	555	650	710
		200	625	725	785
	0,12	50	260	290	400
		75	340	380	500
		100	390	460	600
		125	450	540	675
		150	500	600	750
		200	575	680	-
17,5 {73,5}	0,01	25	355	385	410
		50	430	450	465
		75	460	475	480
		100	475	480	485
		125	480	485	490
		150	485	490	495
		200	485	495	500
		400	490	500	500
	0,02	50	460	515	550
		75	530	570	595
		100	565	600	615
		125	595	610	630
		150	610	620	635
		200	625	635	645
		400	635	645	645
	0,04	50	450	515	575
		75	545	600	655
		100	600	660	705
		125	650	700	740
	0,06	25	255	300	370
		50	390	455	550
		75	490	555	635
		100	565	620	710
		125	620	670	750
	0,08	50	345	435	490
		75	440	530	600
		100	500	605	670
		125	565	650	740
		150	615	705	765
	0,12	25	160	200	275
		50	275	330	450
		75	350	430	530
		100	425	505	630
		125	475	575	725
		150	525	645	775
		200	600	725	-

q	$A\sqrt{h}/A_t$	F_s/V_s	$T_{s,max}$ ε_r 0.3	ε_r 0.5	ε_r 0.7
20 {84}	0,01	25	390	425	445
		50	465	480	490
		75	485	500	500
		100	495	505	505
		125	500	505	510
		150	505	510	510
		200	505	510	515
		400	510	515	515
	0,02	50	500	550	575
		75	560	600	620
		100	595	620	630
		125	615	630	640
		150	625	640	645
		200	635	645	650
		400	650	650	650
	0,04	50	495	565	625
		75	585	630	700
		100	650	700	740
	0,06	25	285	340	415
		50	440	505	600
		75	540	610	700
		100	615	675	735
	0,08	50	390	490	550
		75	485	590	670
		100	565	670	735
		125	630	715	790
	0,12	25	200	235	305
		50	310	375	500
		75	425	480	610
		100	490	560	700
		125	550	620	775
		150	600	685	-
22,5 {94,5}	0,01	25	430	480	480
		50	490	505	515
		75	510	515	520
		100	520	520	720
		125	520	525	525
		150	525	525	525
		200	530	530	530
		400	530	530	530
	0,02	50	530	575	605
		75	590	620	635
		100	615	635	650
		125	630	645	650
		150	645	650	655
		200	650	660	665
	0,04	50	525	600	660
		75	620	690	735
		100	680	740	780
	0,06	25	320	380	460
		50	480	550	645
		75	585	650	740
		100	655	725	785
	0,08	50	430	540	605
		75	540	650	725
		100	610	730	780
	0,12	25	215	255	350
		50	360	415	540
		75	465	540	650
		100	540	615	750
		125	625	675	800
		150	650	740	-

q	$A\sqrt{h}/A_t$	F_s/V_s	$T_{s,max}$ ε_r 0.3	ε_r 0.5	ε_r 0.7
25 {105}	0,01	25	455	490	500
		50	510	525	530
		75	525	530	535
		100	530	535	535
		125	530	535	540
		150	535	540	540
		300	535	540	540
		400	540	540	540
	0,02	50	555	600	625
		75	610	640	650
		100	640	650	655
		125	650	655	660
	0,04	50	570	645	700
		75	650	720	760
	0,06	25	355	420	510
		50	525	600	700
		75	640	690	750
	0,08	50	480	590	655
		75	590	700	770
		100	660	775	-
	0,12	25	240	290	385
		50	400	480	590
		75	500	580	700
		100	590	655	800
		125	650	720	-
30 {126}	0,01	25	505	525	540
		50	545	555	560
		75	555	560	560
		100	560	560	560
		125	560	565	565
		150	560	565	565
		300	565	565	570
		400	565	570	570
	0,02	50	600	640	660
		75	650	670	670
		100	660	675	675
	0,04	50	630	705	750
		75	710	780	800
	0,06	25	410	500	580
		50	595	680	760
		75	705	775	-
	0,08	50	565	665	745
		75	660	775	-
	0,12	25	290	-	440
		50	460	540	650
		75	590	660	770
		100	665	740	-
45 {190}	0,12	25	425	500	640
		50	640	760	-
	0,30	25	210	270	325
		50	360	440	520
		75	430	555	640
		100	535	650	730
		125	595	735	790
90 {380}	0,30	25	425	545	635
		50	650	790	890
		75	790	-	-

Table 3. Maximum steel temperature $T_{s,max}$ (^{o}C) for insulated steel structure as a function of fictitious fire load density q ($Mcal \cdot m^{-2}$) {$MJ \cdot m^{-2}$}, fictitious opening factor $A\sqrt{h}/A_t$ ($m^{1/2}$), structural parameter A_i/V_s (m^{-1}), and insulation parameter d_i/λ_i ($m^2 \cdot {}^{o}C \cdot h \cdot kcal^{-1}$)[a]. d_i denotes insulation thickness (m) [4]

q	$A\sqrt{h}/A_t$	A_i/V_s	$T_{s,max}$ d_i/λ_i 0,05	0,10	0,20	0,30
15 {63}	0,01	100	380	325	255	215
		125	405	350	280	240
		150	420	365	300	260
		200	440	395	335	290
		300	460	430	375	335
		400	470	445	405	370
	0,02	100	390	300	220	180
		125	420	340	250	205
		150	450	360	275	225
		200	500	400	310	260
		300	550	460	370	320
		400	575	505	415	355
	0,04	125	373	270	195	155
		150	400	300	210	175
		200	430	350	250	205
		300	530	420	310	255
		400	600	475	365	300
	0,06	150	350	250	175	140
		200	400	295	210	170
		300	480	370	280	210
		400	540	420	305	245
	0,08	200	350	255	185	145
		300	423	335	225	180
		400	500	390	270	200
	0,12	300	330	250	175	140
		400	350	300	200	165
20 {84}	0,01	75	420	355	280	235
		100	440	385	315	270
		125	460	415	340	290
		150	475	430	365	320
		200	490	455	395	355
		300	500	480	440	400
		400	505	490	460	430
	0,02	75	400	315	240	190
		100	450	355	270	220
		125	480	390	300	250
		150	510	415	325	275
		200	550	470	370	310
		300	595	530	435	370
		400	615	560	475	410
	0,04	100	400	300	210	160
		125	450	340	240	190
		150	490	365	260	210
		200	540	420	310	250
		300	620	500	380	310
		400	670	555	440	360
	0,06	100	350	250	175	135
		125	390	280	200	155
		150	430	320	220	175
		200	490	370	280	210
		300	580	450	325	260
		400	640	505	380	310
	0,08	125	340	240	165	125
		150	370	280	185	150
		200	440	310	225	175
		300	530	400	280	215
		400	600	450	340	260
	0,12	200	360	250	180	140
		300	420	305	215	175
		400	460	365	250	200

q	$A\sqrt{h}/A_t$	A_i/V_s	$T_{s,max}$ d_i/λ_i 0,05	0,10	0,20	0,30
25 {105}	0,01	50	430	360	275	230
		75	470	410	330	275
		100	495	445	370	320
		125	505	465	395	350
		150	515	480	420	375
		200	525	500	450	410
		400	535	530	505	480
	0,02	50	395	300	225	180
		75	455	360	280	230
		100	500	405	310	260
		125	540	445	350	300
		150	560	470	375	320
		200	595	515	420	360
		300	635	570	490	435
		400	650	605	525	470
	0,04	75	400	295	200	160
		100	450	350	240	195
		125	510	380	270	220
		150	550	420	300	250
		200	600	480	350	290
		300	680	555	425	365
		400	725	615	485	420
	0,06	75	350	245	170	130
		100	410	295	200	160
		125	455	330	230	185
		150	500	370	255	205
		200	565	430	310	245
		300	655	520	380	305
		400	710	580	440	360
	0,08	100	350	255	175	140
		125	400	290	195	155
		150	450	325	220	175
		200	500	380	260	210
		300	600	470	340	265
		400	675	540	390	315
	0,12	150	360	245	175	140
		200	430	300	210	165
		300	510	370	260	210
		400	570	430	300	240
30 {126}	0,01	25	390	310	225	180
		50	480	410	320	270
		75	515	460	380	315
		100	535	490	420	365
		125	540	510	450	400
		150	550	525	470	425
		200	555	535	500	460
		400	560	555	540	520
	0,02	25	325	240	165	130
		50	440	345	250	200
		75	510	405	305	250
		100	550	450	350	290
		125	580	490	385	325
		150	605	520	420	355
		200	630	560	470	400
		300	665	610	540	470
		400	675	640	570	515
	0,04	50	370	270	185	140
		75	450	340	240	185
		100	510	400	280	220
		125	560	440	310	250
		150	600	475	350	285
		200	660	540	400	330
		300	730	615	485	405
		400	760	670	540	460
	0,06	75	395	280	190	150
		100	460	335	230	180
		125	510	375	265	210
		150	550	415	290	235
		200	620	475	345	275
		300	710	570	425	350
		400	765	635	490	405
	0,08	75	350	245	170	130
		100	410	295	200	160
		125	455	330	230	180
		150	500	370	255	205
		200	570	425	300	245
		300	670	525	390	305
		400	740	600	450	365
	0,12	100	340	240	155	125
		125	375	260	175	140
		150	420	290	200	160
		200	500	350	240	190
		300	600	440	300	250
		400	675	500	350	290

q	$A\sqrt{h}/A_t$	A_i/V_s	$T_{s,max}$ d_i/λ_i 0,05	0,10	0,20	0,30
35 {147}	0,02	25	360	260	185	145
		50	490	380	270	225
		75	550	445	340	280
		100	595	490	385	325
		125	625	535	425	360
		150	645	555	460	395
		200	665	600	510	445
		300	690	640	580	515
		400	700	670	610	560
	0,04	25	275	200	130	100
		50	410	300	205	160
		75	500	380	265	210
		100	560	440	310	250
		125	610	480	350	280
		150	650	525	385	310
		200	700	590	445	370
		300	760	665	530	450
		400	-	710	585	510
	0,06	50	350	250	165	125
		75	430	320	215	170
		100	500	370	255	200
		125	555	415	295	235
		150	595	455	320	260
		200	660	520	380	305
		300	750	610	465	380
		400	800	675	530	440
	0,08	75	380	275	185	145
		100	450	325	220	175
		125	500	365	255	200
		150	540	405	280	225
		200	610	470	340	265
		300	715	570	430	345
		400	-	640	490	400
	0,12	100	375	265	170	135
		125	420	290	195	155
		150	465	325	225	180
		200	545	390	265	210
		300	645	480	335	275
		400	705	545	390	315
40 {168}	0,02	25	400	300	210	165
		50	530	425	310	250
		75	595	495	380	315
		100	635	545	435	360
		125	665	580	480	400
		150	680	610	510	435
		200	700	645	560	490
		300	720	680	625	550
		400	725	700	650	600
	0,04	25	300	220	145	115
		50	445	330	225	180
		75	525	400	290	235
		100	595	465	340	270
		125	645	510	380	310
		150	680	550	420	340
		200	730	615	475	395
		300	790	695	565	480
		400	-	740	630	545
	0,06	50	385	275	185	140
		75	475	350	235	185
		100	540	405	280	225
		125	595	450	325	255
		150	640	490	355	285
		200	705	560	415	335
		300	790	660	500	415
		400	-	720	565	480
	0,08	50	340	240	155	120
		75	425	300	205	160
		100	500	355	250	195
		125	550	400	280	220
		150	600	450	310	250
		200	675	505	370	300
		300	760	600	470	380
		400	-	690	530	445
	0,12	75	340	240	160	120
		100	410	290	185	145
		125	465	320	215	170
		150	510	360	250	200
		200	590	430	290	235
		300	690	520	370	300
		400	735	590	430	350

q	$A\sqrt{h}/A_t$	A_i/V_s	$T_{s,max}$ d_i/λ_i 0,05	0,10	0,20	0,30
45 {190}	0,02	25	445	330	230	180
		50	570	460	340	275
		75	640	540	415	340
		100	670	580	470	395
		125	695	620	510	440
		150	710	650	550	475
		200	725	680	600	530
		300	740	710	655	600
		400	745	730	680	640
	0,04	25	330	245	160	125
		50	480	350	250	195
		75	565	440	315	250
		100	630	500	370	300
		125	680	550	410	340
		150	715	590	450	370
		200	765	630	510	430
		300	-	725	600	510
		400	-	770	653	580
	0,06	25	280	195	125	95
		50	420	300	200	155
		75	510	380	260	205
		100	585	440	310	245
		125	640	490	350	280
		150	685	530	390	310
		200	750	600	450	370
		300	-	700	540	455
		400	-	765	610	520
	0,08	50	375	260	175	135
		75	465	335	225	180
		100	530	395	270	210
		125	590	445	305	240
		150	640	490	340	275
		200	710	550	395	315
		300	800	650	500	400
		400	-	725	555	475
	0,12	75	370	260	170	130
		100	445	315	200	155
		125	510	350	235	185
		150	555	395	275	220
		200	635	470	320	260
		300	735	560	405	325
		400	790	635	470	385
	0,30	150	325	215	140	115
		200	385	265	170	135
		300	475	340	225	175
		400	545	400	270	210

[a] {0,05 m² °Ch/kcal = 0,043 m² °C/W
0,10 » = 0,086 »
0,20 » = 0,172 »
0,30 » = 0,258 »}

q	$\frac{A\sqrt{h}}{A_t}$	$\frac{A_i}{V_s}$	$T_{s,max}$ d_i/λ_i 0,05	d_i/λ_i 0,10	d_i/λ_i 0,20	d_i/λ_i 0,30
50 (210)	0,02	25	480	355	250	200
		50	605	490	375	300
		75	665	570	450	380
		100	700	620	510	435
		125	720	650	550	475
		150	730	675	585	510
		200	745	700	630	565
		300	755	735	680	635
	0,04	25	350	255	170	135
		50	500	385	270	210
		75	600	460	340	265
		100	655	525	395	315
		125	705	575	435	355
		150	740	615	475	395
		200	785	675	540	450
		300	-	750	625	545
		400	-	795	690	600
	0,06	25	300	210	135	105
		50	445	320	215	170
		75	540	400	275	220
		100	610	465	330	260
		125	663	515	375	300
		150	710	560	410	330
		200	775	625	475	395
		300	-	725	570	480
		400	-	790	635	545
	0,08	25	260	180	115	90
		50	400	275	180	140
		75	500	350	240	190
		100	555	410	290	225
		125	615	460	325	255
		150	665	505	355	295
		200	750	580	425	350
		300	-	680	525	430
		400	-	750	595	500
	0,12	50	320	220	145	110
		75	410	290	185	145
		100	480	345	225	175
		125	550	390	260	200
		150	600	430	295	235
		200	675	500	350	280
		300	780	600	440	350
		400	-	680	510	415
	0,30	125	305	205	135	110
		150	350	230	150	125
		200	410	285	185	145
		300	500	365	245	190
		400	575	425	290	225

q	$\frac{A\sqrt{h}}{A_t}$	$\frac{A_i}{V_s}$	$T_{s,max}$ d_i/λ_i 0,05	d_i/λ_i 0,10	d_i/λ_i 0,20	d_i/λ_i 0,30
60 (250)	0,02	25	550	420	295	235
		50	665	560	430	350
		75	715	640	515	435
		100	745	675	570	495
		125	760	705	610	540
		150	770	725	640	575
		200	780	750	690	625
	0,04	25	405	300	200	150
		50	560	430	305	240
		75	650	515	380	310
		100	715	580	440	360
		125	755	640	490	405
		150	790	675	530	440
		200	-	730	600	505
		300	-	795	680	590
	0,06	25	345	240	155	120
		50	500	360	240	195
		75	600	450	315	250
		100	670	515	375	300
		125	725	570	415	340
		150	765	615	460	375
		200	-	685	525	435
		300	-	775	625	530
		400	-	-	695	600
	0,08	25	300	200	135	100
		50	450	315	210	160
		75	550	400	275	210
		100	615	460	325	255
		125	680	515	365	290
		150	725	560	400	330
		200	800	640	475	390
		300	-	750	580	480
		400	-	-	650	550
	0,12	50	370	250	160	125
		75	470	330	210	170
		100	550	385	250	200
		125	600	430	300	235
		150	650	480	330	265
		200	735	550	400	310
		300	-	660	500	400
		400	-	750	575	465
	0,30	125	345	235	155	125
		150	395	265	175	145
		200	460	325	215	165
		300	555	410	280	220
		400	630	475	330	260

q	$\frac{A\sqrt{h}}{A_t}$	$\frac{A_i}{V_s}$	$T_{s,max}$ d_i/λ_i 0,05	d_i/λ_i 0,10	d_i/λ_i 0,20	d_i/λ_i 0,30
75 (315)	0,04	25	525	395	270	205
		50	665	540	400	320
		75	735	625	490	400
		100	790	680	550	455
		125	-	710	600	505
		150	-	750	640	550
		200	-	800	695	605
	0,06	25	400	280	185	140
		50	565	415	285	225
		75	670	510	365	290
		100	740	585	425	345
		125	790	640	480	390
		150	-	685	525	430
		200	-	755	595	500
		300	-	-	695	600
	0,08	25	350	240	160	120
		50	510	365	250	190
		75	615	455	320	250
		100	700	530	375	300
		125	750	585	425	340
		150	800	640	470	385
		200	-	710	545	450
		300	-	-	650	550
		400	-	-	730	625
	0,12	50	420	290	190	150
		75	525	375	250	200
		100	600	440	300	240
		125	680	500	350	275
		150	725	550	390	300
		200	800	620	450	360
		300	-	730	550	450
		400	-	800	650	530
	0,30	75	305	205	135	105
		100	365	250	165	130
		125	410	285	190	150
		150	465	315	210	170
		200	535	385	255	200
		300	635	480	335	260
		400	715	550	390	310

q	$\frac{A\sqrt{h}}{A_t}$	$\frac{A_i}{V_s}$	$T_{s,max}$ d_i/λ_i 0,05	d_i/λ_i 0,10	d_i/λ_i 0,20	d_i/λ_i 0,30
90 (380)	0,04	25	630	480	330	260
		50	760	640	490	395
		75	-	725	590	490
		100	-	770	650	560
		125	-	790	700	610
		150	-	-	730	650
	0,06	25	450	315	210	160
		50	625	470	325	255
		75	730	570	410	330
		100	795	640	475	390
		125	-	700	530	435
		150	-	745	575	480
		200	-	-	650	550
		300	-	-	750	665
	0,08	25	400	275	180	140
		50	570	415	285	220
		75	680	510	360	285
		100	755	590	420	340
		125	-	650	480	390
		150	-	700	520	430
		200	-	775	600	500
		300	-	-	700	600
	0,12	25	320	220	140	105
		50	475	330	220	175
		75	590	425	285	225
		100	670	495	340	275
		125	740	550	395	305
		150	800	600	440	350
		200	-	680	500	405
		300	-	800	605	505
		400	-	-	700	595
	0,30	75	353	245	160	125
		100	425	290	195	150
		125	480	335	225	175
		150	530	375	250	195
		200	610	445	300	235
		300	720	545	385	305
		400	800	625	455	360

q	$\frac{A\sqrt{h}}{A_t}$	$\frac{A_i}{V_s}$	$T_{s,max}$ d_i/λ_i 0,05	d_i/λ_i 0,10	c_i/λ_i 0,20	d_i/λ_i 0,30
120 (500)	0,04	25	660	500	350	270
		50	-	670	520	420
		75	-	760	620	520
		100	-	-	695	595
		125	-	-	745	650
	0,06	25	550	395	265	200
		50	735	570	400	320
		75	-	675	500	405
		100	-	750	575	475
		125	-	800	635	535
		150	-	-	685	580
		200	-	-	733	653
	0,08	25	475	325	220	165
		50	660	490	340	260
		75	770	595	435	340
		100	-	670	505	400
		125	-	740	560	450
		150	-	780	610	500
		200	-	-	690	580
	0,12	25	390	250	165	130
		50	565	390	260	210
		75	690	495	340	270
		100	760	565	400	320
		125	-	640	450	370
		150	-	690	500	410
		200	-	760	575	480
		300	-	-	700	590
	0,30	75	435	300	195	150
		100	510	355	235	180
		125	575	410	270	210
		150	625	455	305	240
		200	705	530	365	285
		300	-	640	465	370
		400	-	720	540	435

Table 4. Maximum steel temperature $T_{s,max}$ (^{o}C) for a steel structure insulated with gypsum plaster slabs, type Gyproc (ρ_i = 790 kg·m^{-3}), as a function of fictitious fire load density q (Mcal·m^{-2}){MJ·m^{-2}}, fictitious opening factor $A\sqrt{h}/A_t$ ($m^{1/2}$), structural parameter A_i/V_s (m^{-1}), and insulation thickness d_i (mm) [4]

q	$A\sqrt{h}/A_t$	A_i/V_s	$T_{s,max}$ d_i 13	$T_{s,max}$ d_i 26
15 {63}	0,01	125	315	200
		150	335	215
		200	365	235
		300	395	260
		400	415	275
	0,02	125	300	150
		150	325	165
		200	350	200
		300	405	215
		400	435	230
	0,04	300	300	120
		400	330	125
20 {84}	0,01	75	345	230
		100	380	260
		125	405	280
		150	420	300
		200	440	325
		300	465	355
		400	480	375
	0,02	75	300	180
		100	345	200
		125	375	220
		150	400	235
		200	440	265
		300	490	300
		400	520	320
	0,04	125	300	130
		150	325	140
		200	370	155
		300	435	175
		400	475	200
	0,06	300	300	110
		300	350	115
		400	400	120
	0,08	300	295	100
		400	320	110
25 {105}	0,01	50	360	250
		75	410	300
		100	440	335
		125	470	360
		150	480	375
		200	500	410
		300	520	440
		400	530	465
	0,02	50	300	175
		75	355	225
		100	400	255
		125	430	285
		150	455	300
		200	500	335
		300	550	375
		400	585	400
	0,04	100	335	150
		125	375	180
		150	400	200
		200	455	225
		300	550	260
		400	600	295
	0,06	125	300	130
		150	330	135
		200	375	150
		300	415	175
		400	500	195
	0,08	200	320	115
		300	370	120
		400	410	130

q	$A\sqrt{h}/A_t$	A_i/V_s	$T_{s,max}$ d_i 13	$T_{s,max}$ d_i 26
30 {126}	0,01	25	315	210
		50	415	305
		75	465	360
		100	495	395
		125	510	420
		150	525	440
		200	535	465
		300	550	495
		400	560	510
	0,02	50	350	215
		75	410	265
		100	460	305
		125	495	335
		150	520	365
		200	570	400
		300	640	450
		400	685	470
	0,04	75	345	185
		100	400	215
		125	435	245
		150	470	260
		200	520	300
		300	630	350
		400	695	380
	0,06	100	330	140
		125	365	155
		150	395	175
		200	445	200
		300	550	235
		400	600	255
	0,08	125	305	120
		150	345	125
		200	390	135
		300	450	153
		400	500	170
	0,12	300	330	120
		400	380	125
35 {147}	0,02	50	390	255
		75	465	305
		100	520	345
		125	560	380
		150	595	420
		200	640	490
		300	690	540
		400	705	570
	0,04	50	310	170
		75	385	230
		100	445	265
		125	490	295
		150	535	315
		200	600	355
		300	710	425
		400	775	475
	0,06	75	320	150
		100	375	175
		125	415	190
		150	440	215
		200	430	245
		300	640	290
		400	700	315
	0,08	100	315	140
		125	355	150
		150	395	160
		200	450	180
		300	520	220
		400	590	245
	0,12	200	340	120
		300	390	130
		400	450	135

q	$A\sqrt{h}/A_t$	A_i/V_s	$T_{s,max}$ d_i 13	$T_{s,max}$ d_i 26
40 {168}	0,02	25	305	195
		50	435	290
		75	525	345
		100	600	390
		125	640	425
		150	675	500
		200	700	585
		300	720	650
	0,04	50	350	200
		75	425	260
		100	485	300
		125	535	325
		150	605	353
		200	690	400
		300	780	495
		400	-	560
	0,06	75	365	185
		100	420	215
		125	450	235
		150	485	260
		200	600	300
		300	730	355
		400	800	385
	0,08	75	305	160
		100	360	185
		125	400	200
		150	445	220
		200	510	250
		300	600	295
		400	665	325
	0,12	125	315	115
		150	350	120
		200	400	135
		300	450	145
		400	540	155
45 {190}	0,02	25	330	225
		50	495	335
		75	600	405
		100	685	435
		125	715	500
		150	740	600
	0,04	50	380	230
		75	460	290
		100	525	330
		125	585	385
		150	675	400
		200	775	445
		300	-	555
		400	-	650
	0,06	50	320	175
		75	400	220
		100	460	253
		125	505	290
		150	540	315
		200	670	360
		300	-	425
		400	-	450
	0,08	75	340	200
		100	400	230
		125	445	250
		150	495	265
		200	585	310
		300	685	350
		400	760	400
	0,12	100	305	125
		125	345	125
		150	375	130
		200	420	155
		300	500	170
		400	615	175

q	$A\sqrt{h}/A_t$	A_i/V_s	$T_{s,max}$ d_i 13	$T_{s,max}$ d_i 26
50 {210}	0,02	25	390	250
		50	550	370
		75	635	500
		100	725	570
		125	755	615
		150	765	680
	0,04	50	410	275
		75	500	330
		100	575	380
		125	650	420
		150	745	455
		200	-	500
		300	-	635
	0,06	50	350	205
		75	435	265
		100	510	310
		125	570	345
		150	600	375
		200	750	425
		300	-	495
		400	-	535
	0,08	50	300	200
		75	375	245
		100	440	280
		125	490	300
		150	550	330
		200	650	375
		300	770	415
		400	-	500
	0,12	100	340	145
		125	385	150
		150	420	165
		200	470	200
		300	575	220
		400	735	230
	0,30	300	220	100
		400	260	105
60 {250}	0,02	25	465	320
		50	690	450
		75	770	680
	0,04	25	325	265
		50	470	390
		75	575	455
		100	730	520
		125	-	595
		150	-	660
	0,06	50	400	295
		75	490	375
		100	610	425
		125	710	450
		150	760	490
		200	-	600
	0,08	50	350	250
		75	435	315
		100	500	365
		125	555	400
		150	650	440
		200	780	500
		300	-	550
		400	-	660
	0,12	75	340	195
		100	400	220
		125	450	250
		150	500	280
		200	575	320
		300	690	355
		400	-	400
	0,30	300	300	105
		400	325	120

q	$A\sqrt{h}/A_t$	A_i/V_s	$T_{s,max}$ d_i 13	$T_{s,max}$ d_i 26
73 {315}	0,04	25	395	350
		50	620	535
		75	735	650
	0,06	25	315	265
		50	465	390
		75	590	475
		100	775	550
		125	-	630
		150	-	675
	0,08	50	410	325
		75	525	400
		100	630	480
		125	700	535
		150	-	595
		200	-	675
	0,12	50	320	230
		75	400	300
		100	475	350
		125	540	375
		150	650	410
		200	765	450
		300	-	565
		400	-	655
	0,30	150	300	115
		200	325	115
		300	395	125
		400	435	150
90 {380}	0,04	25	470	415
		50	800	665
	0,06	25	365	310
		50	530	450
		75	785	550
		100	-	720
	0,08	25	315	260
		50	470	395
		75	625	485
		100	800	550
		125	-	665
	0,12	50	375	300
		75	465	375
		100	550	440
		125	650	480
		150	800	525
		200	-	600
		300	-	800
		400	-	-
	0,30	100	295	115
		125	325	125
		150	360	135
		200	400	140
		300	480	170
		400	550	200
120 {500}	0,04	25	690	550
		50	-	-
	0,06	25	465	410
		50	760	680
	0,08	25	390	345
		50	610	510
		75	-	710
	0,12	25	305	255
		50	470	390
		75	665	500
		100	800	600
		125	-	710
	0,30	75	325	180
		100	380	220
		125	435	250
		150	475	275
		200	560	295
		300	745	350
		400	-	395

Table 5. Maximum steel beam temperature $T_{s,max}$ (^{o}C) for a steel beam construction according to Fig. 10, with an insulation in the form of a suspended ceiling, as a function of fictitious fire load density q ($Mcal \cdot m^{-2}$){$MJ \cdot m^{-2}$}, fictitious opening factor $A\sqrt{h}/A_t$ ($m^{1/2}$), structural parameter F_s/V_s (m^{-1}), and insulation parameter d_i/λ_i ($m^2 \cdot {}^{o}C \cdot h \cdot kcal^{-1}$)[c]. The maximum temperature in the suspended ceiling is given in brackets [4]

q	$A\sqrt{h}/A_t$	F_s/V_s	Maximum steel temperature $T_{s,max}$ and ( ) maximum suspended ceiling temperature $(d_i/\lambda_i)_{fict}$ 0,05	0,10	0,20	0,30
15 {63}	0,02	50	130	90	65	50
		100	180 (470)	130 (440)	90 (410)	70 (390)
		200	230	170	115	90
		300	260	190	130	100
	0,04	50	100	70	45	40
		100	150 (565)	100 (530)	65 (500)	50 (475)
		200	200	140	90	70
		300	240	170	110	80
	0,08	50	65	50	35	25
		100	95 (675)	70 (630)	50 (590)	40 (570)
		200	150	100	65	50
		300	190	125	90	60
	0,12	50	40	35	30	25
		100	60 (735)	45 (690)	40 (650)	30 (620)
		200	120	70	50	40
		300	155	100	60	45
25 {105}	0,02	50	200	140	95	75
		100	260 (510)	185 (470)	125 (435)	100 (420)
		200	300	225	155	120
		300	320	245	170	130
	0,04	50	160	110	75	55
		100	230 (600)	150 (565)	100 (530)	75 (515)
		200	290	205	135	100
		300	325	235	155	115
	0,08	50	115	75	50	40
		100	160 (680)	110 (635)	70 (595)	55 (570)
		200	240	160	100	75
		300	285	195	120	90
	0,12	50	80	60	40	30
		100	130 (740)	80 (690)	60 (650)	45 (620)
		200	190	125	80	60
		300	235	160	100	75
40 {168}	0,02	50	300	220	145	110
		100	360 (560)	260 (520)	175 (480)	135 (460)
		200	380	290	200	160
		300	385	295	210	165
	0,04	50	240	160	105	80
		100	315 (645)	220 (600)	140 (560)	100 (535)
		200	375	270	180	135
		300	390	290	195	150
	0,08	50	170	110	70	55
		100	245 (715)	160 (665)	100 (625)	75 (600)
		200	335	220	140	105
		300	380	260	165	120
	0,12	50	130	85	55	45
		100	200 (750)	130 (700)	85 (660)	60 (630)
		200	290	190	115	85
		300	340	225	145	100

q	$A\sqrt{h}/A_t$	F_s/V_s	Maximum steel temperature $T_{s,max}$ and( ) maximum suspended ceiling temperature $(d_i/\lambda_i)_{fict}$ 0,05	0,10	0,20	0,30
60 {250}	0,02	50	435	315	200	160
		100	450 (615)	340 (570)	240 (530)	185 (500)
		200	455	350	250	200
		300	455	350	250	200
	0,04	50	340	225	145	110
		100	400 (680)	285 (630)	185 (590)	140 (560)
		200	435	320	220	165
		300	445	330	230	180
	0,08	50	250	160	100	75
		100	340 (750)	225 (700)	130 (650)	100 (625)
		200	415	285	185	135
		300	445	315	210	155
	0,12	50	190	120	75	60
		100	285 (780)	185 (725)	110 (680)	80 (660)
		200	375	250	155	110
		300	420	290	185	130
90 {380}	0,04	50	475	330	205	150
		100	510 (740)	370 (680)	250 (630)	190 (600)
		200	515	385	270	210
		300	515	385	270	215
	0,08	50	345	225	130	100
		100	430 (790)	290 (730)	180 (675)	130 (650)
		200	480	340	225	170
		300	495	360	250	190
120 {500}	0,04	50	560	400	260	200
		100	570 (780)	420 (715)	290 (660)	220 (630)
		200	575	425	300	230
		300	575	425	300	230
	0,08	50	425	280	160	120
		100	495 (810)	345 (750)	210 (695)	160 (670)
		200	520	375	250	195
		300	525	385	260	205

[c] 0,05 $m^2 \cdot {}^{o}Ch/kcal$ = 0,043 $m^2 \cdot {}^{o}C/W$
0,10 » = 0,086 »
0,20 » = 0,172 »
0,30 » = 0,258 »

Table 6. Summary results of standard fire resistance tests on some types of suspended ceilings and connected values, derived from the test results, for $(d_i/\lambda_i)_{fict}$ and critical temperature of the ceilings [4]

No	Make	Material	Resistance time in standard fire test (min)	Remarks	Estimated $(d_i/\lambda_i)_{fict}$ $\left(\frac{m^2\,°Ch}{kcal}\right)$	$\left(\frac{m^2\,°C}{W}\right)$	Estimated critical suspended ceiling temperature (°C)
1	Gyproc	2x13 mm gypsum plaster slabs no glass fibre reinforcement	30-40	All tests were discontinued because the suspended ceiling fell down. The critical temperature had not been reached in the steel girders	0,075	0,064	625
2		1x13 mm gypsum plaster slabs 0.25% g f r	48		0,075	0,064	650
3		1x16 mm gypsum plaster slabs 0.25% g f r	49		0,10	0,086	650
4		2x13 mm gypsum plaster slabs 0.25% g f r	60		0,15	0,129	650
5		3x13mm gypsum plaster slabs 0.25% g f r	75-80		0,25	0,215	625
6		2x20 mm gypsum plaster slabs 0.25% g f r	80		0,30	0,258	625
7	WST	2x13 mm gypsum plaster slabs with 13 mm mineral wool between them	45	All tests were discontinued for the same reason as above. The gypsum plaster slabs were not reinforced	0,30	0,258	550
8		2x13 mm gypsum plaster slabs with 13 mm mineral wool between them	50		0,30	0,258	550
9		2x13 mm gypsum plaster slabs with 43 mm straw between them	47		0,30	0,258	550
10		2x13mm gypsum plaster slabs with 43 mm straw between them	54		0,30	0,258	550
11	Ingenjörs-firma Zero	Soundex special suspended ceiling tiles. Cast glass fibre reinforced gypsum plaster tiles with "ridges" in a grid pattern. Tile thickness 18 mm, at the ridges 38 mm	90	Parts of the ceiling fell down after 90 minutes. Max. steel temperature approx. 440°C	0,15	0,129	700
12	Consentus	Armstrong 13 mm thick	30	No visible damage to suspended ceiling. Max steel temperature about 450 °C	0,05	0,043	550
13		Mineral wool acoustic 16 mm thick	80		0,075	0,064	>(725)[a]
14		Type minaboard 13 mm thick	85		0,075	0,064	>(725)[a]
15	Dansk Eternitfabrik	Deflamit-Asbestolux (9 mm Deflamit + 15 mm mineral wool + 9 mm eternit)	90	No visible damage to suspended ceiling. Max steel temperature about 300 °C	0,20	0,172	>(879)[a]
16	Nordakustik	Celotex Acoustiformat 15 mm thick glass fibre slab	90	No visible damage to suspended ceiling. Max steel temperature about 450 °C. The test was discontinued because the suspended ceiling fell down. The critical temperature had not been reached in the steel girders.	0,10	0,086	(725)[a]
17	Rockwool	Rockfon Decor 851 (15 mm thick mineral wool slab)	66		0,20	0,172	600

[a] No damage to the suspended ceiling. Calculated temperature in the suspended ceiling when the test was discontinued.